



HAL
open science

Structure-Directing Effects of Counterions in Uranyl Ion Complexes with Long-Chain Aliphatic α,ω -Dicarboxylates: 1D to Polycatenated 3D Species

Pierre Thuéry, Youssef Atoini, Jack Harrowfield

► To cite this version:

Pierre Thuéry, Youssef Atoini, Jack Harrowfield. Structure-Directing Effects of Counterions in Uranyl Ion Complexes with Long-Chain Aliphatic α,ω -Dicarboxylates: 1D to Polycatenated 3D Species. *Inorganic Chemistry*, 2018, 58, pp.567-580. cea-01965731

HAL Id: cea-01965731

<https://cea.hal.science/cea-01965731>

Submitted on 26 Dec 2018

HAL is a multi-disciplinary open access archive for the deposit and dissemination of scientific research documents, whether they are published or not. The documents may come from teaching and research institutions in France or abroad, or from public or private research centers.

L'archive ouverte pluridisciplinaire **HAL**, est destinée au dépôt et à la diffusion de documents scientifiques de niveau recherche, publiés ou non, émanant des établissements d'enseignement et de recherche français ou étrangers, des laboratoires publics ou privés.

Structure-Directing Effects of Counterions in Uranyl Ion Complexes with Long-Chain Aliphatic α,ω -Dicarboxylates: 1D to Polycatenated 3D Species

Pierre Thuéry,^{*,†} Youssef Atouini[‡] and Jack Harrowfield^{*,‡}

[†]NIMBE, CEA, CNRS, Université Paris-Saclay, CEA Saclay 91191 Gif-sur-Yvette, France

[‡]ISIS, Université de Strasbourg, 8 allée Gaspard Monge, 67083 Strasbourg, France

ABSTRACT: Nine uranyl ion complexes were synthesized under (solvo-)hydrothermal conditions using α,ω -dicarboxylic acids $\text{HOOC}-(\text{CH}_2)_{n-2}-\text{COOH}$ (H_2C_n , $n = 6-9$) and diverse counterions. Complexes $[\text{PPh}_4][\text{UO}_2(\text{C6})(\text{NO}_3)]$ (**1**) and $[\text{PPh}_4][\text{UO}_2(\text{C8})(\text{NO}_3)]$ (**2**) contain zigzag one-dimensional (1D) chains, further polymerization being prevented by the terminal nitrate ligands. $[\text{PPh}_3\text{Me}][\text{UO}_2(\text{C7})(\text{HC7})]$ (**3**) crystallizes as a 1D polymer with a curved section, hydrogen bonding of the uncomplexed carboxylic groups giving rise to formation of threefold interpenetrated two-dimensional (2D) networks. $[\text{PPh}_4][\text{H}_2\text{NMe}_2][(\text{UO}_2)_2(\text{C7})_3]$ (**4**) and $[\text{PPh}_3\text{Me}]_2[(\text{UO}_2)_2(\text{C8})_3]$ (**5**) contain 1D chains, either ladderlike or containing doubly bridged dimers, while $[\text{PPh}_3\text{Me}]_2[(\text{UO}_2)_2(\text{C9})_3]\cdot 2\text{H}_2\text{O}$ (**6**) displays interdigitated, strongly corrugated honeycomb 2D nets. Ladderlike 1D polymers in $[\text{Cu}(\text{R},\text{S-Me}_6\text{cyclam})][(\text{UO}_2)_2(\text{C7})_2(\text{C}_2\text{O}_4)]\cdot 4\text{H}_2\text{O}$ (**7**) are associated into columns by the hydrogen bonded counterions, whereas the $[\text{Ni}(\text{cyclam})]^{2+}$ moieties are part of the 2D polymeric arrangement in $[(\text{UO}_2)_2(\text{C7})_2(\text{HC7})_2\text{Ni}(\text{cyclam})]\cdot 2\text{H}_2\text{O}$ (**8**) due to axial coordination of the nickel(II) centre, hydrogen bonding mediated by water molecules generating a three-dimensional (3D) net. $[(\text{UO}_2)_2\text{K}_2(\text{C7})_3(\text{H}_2\text{O})]\cdot 0.5\text{H}_2\text{O}$ (**9**) contains convoluted uranyl dicarboxylate 2D subunits which generate a 3D framework through 2D \rightarrow 3D parallel polycatenation similar to that previously found in $[\text{NH}_4]_2[(\text{UO}_2)_2(\text{C7})_3]\cdot 2\text{H}_2\text{O}$; further linking of these subunits is provided by bonding of the potassium cations to carboxylate and uranyl oxido groups. The solid state emission spectra of complexes **1-6** and **9** display maxima positions typical of hexacoordinated uranyl carboxylate complexes, but uranyl luminescence is quenched in **7**. A solid-state photoluminescence quantum yield of 11.5% has been measured for complex **1**, while those for compounds **3-6** and **9** are in the range of 2.0-3.5%.

INTRODUCTION

The aliphatic α,ω -dicarboxylic acids $\text{HOOC}-(\text{CH}_2)_{n-2}-\text{COOH}$ (H_2C_n) in their deprotonated carboxylate form constitute a family of potentially ditopic ligands of variable length and flexibility, in which the relative orientation of the two binding sites can be modulated over a large range. Fully extended chains provide divergent metal ion binding sites which, for large n values, can widely separate metal centres and favour polymer formation, while curved or buckled conformations of the chains may provide more or less convergent ligands compatible with closer locations of the metal centres and, possibly, closed oligomer formation. A consequent problem is that of finding structure-directing species enabling control of the ligand conformation, although unpredictability is obviously a characteristic of such flexible systems. In uranyl ion coordination chemistry, and in particular in the investigation of uranyl–organic coordination polymers,^{1–5} no such control is known in the case of the first two aliphatic dicarboxylates, oxalate ($n = 2$) and malonate ($n = 3$), as these ligands appear to favour simple chelation involving both carboxylate groups, often associated with bridging and polymer formation, and it is yet to be systematically demonstrated whether or not it is possible in the case of the next two members of the series, succinate ($n = 4$) and glutarate ($n = 5$), for which 15 and 20 examples, respectively, are reported in the Cambridge Structural Database (CSD, Version 5.39),⁶ although these are now ligands clearly favouring polymer formation. Uranyl complexes of dicarboxylates with longer chains ($n = 5–10$) have been investigated by Cahill's group, with a particular emphasis on their association with molecules such as 4,4'-bipyridine, 1,2-bis(4-pyridyl)ethane and trans-1,2-bis(4-pyridyl)ethylene, in a deliberate effort to use these large molecules to influence the form of uranyl–dicarboxylate coordination polymers.^{7–9} These bipyridyl species assume the various roles of coligands, counterions, and structure-directing species, depending on their length compared to that of the dicarboxylates. Other diverse species, either neutral such as cucurbiturils,¹⁰ 2,2'-bipyridine (bipy) or 1,10-phenanthroline (phen),¹¹ or

cationic such as NH_4^+ ,¹² H_2NMe_2^+ ,¹³ $[\text{M}(\text{L})_x]^{n+}$, with $\text{M} = \text{Mn, Fe, Co, Ni, Cu, Ag}$, $\text{L} = \text{bipy}$ or phen , $x = 2$ or 3 and $n = 1$ or 2 ,^{12,14–17} $[\text{Co}(\text{en})_3]^{3+}$, with $\text{en} = \text{ethylenediamine}$,¹² or Pb^{2+} ,¹⁷ have also been found to act as structure-directing agents in uranyl ion complexes with C_n^{2-} ($n = 6–10, 12, 13$ and 15), whether they be neutral co-crystallized species, coligands, counterions or additional metal groups included in the polymer. A nice example of control of the uranyl complex geometry through choice of aliphatic chain length and counterion is provided by the isolation of discrete, triple-stranded binuclear helicates $[\text{M}(\text{bipy})_3][(\text{UO}_2)_2(\text{C}_9)_3]$ and $[\text{M}(\text{phen})_3][(\text{UO}_2)_2(\text{C}_{12})_3]$ ($\text{M} = \text{Mn, Co, Ni}$),¹⁴ or of polymeric $[\text{Mn}(\text{phen})_3][(\text{UO}_2)_2(\text{C}_{13})_3]$ species displaying Borromean-type entanglement.¹⁵ Following our recent use of PPh_4^+ and PPh_3Me^+ ,^{18–20} $[\text{Ni}(\text{cyclam})]^{2+}$ and $[\text{Ni}(\text{R,S-Me}_6\text{cyclam})]^{2+}$ ($\text{cyclam} = 1,4,8,11\text{-tetraazacyclotetradecane}$ and $\text{R,S-Me}_6\text{cyclam}$ (meso isomer) = $7(\text{R}),14(\text{S})\text{-}5,5,7,12,12,14\text{-hexamethylcyclam}$)²¹ and alkali metal ion complexes of crown ethers²² as bulky counterions in the synthesis of uranyl-containing coordination polymers with conformationally restricted 1,3-adamantanediacetate and diverse members of the cyclohexanedicarboxylate family, we have attempted to use these or similar counterions along with conformationally labile and flexible C_n^{2-} α,ω -dicarboxylates, and the first results are reported here. Nine complexes including C_6^{2-} to C_9^{2-} and either PPh_4^+ , PPh_3Me^+ , $[\text{Ni}(\text{cyclam})]^{2+}$, $[\text{Cu}(\text{R,S-Me}_6\text{cyclam})]^{2+}$ or simple K^+ ions as counterions to anionic uranyl polymers, have been obtained and characterized by their crystal structure and, in most cases, their emission spectrum and luminescence quantum yield in the solid state. While most of them crystallize as one- or two-dimensional (1D or 2D) coordination polymers, one is a polycatenated three-dimensional (3D) framework, while another provides an example of hydrogen bonded interpenetration. Network entanglements in uranyl chemistry are now well documented,²³ and several examples have been reported recently.^{23–26} It is notable that one of the first cases of polycatenation in a uranyl ion complex was found with C_6^{2-} as ligand,⁸ other cases having later been reported involving C_7^{2-} and C_{13}^{2-} .^{12,15}

EXPERIMENTAL SECTION

Syntheses. Caution! Uranium is a radioactive and chemically toxic element, and uranium-containing samples must be handled with suitable care and protection.

$\text{UO}_2(\text{NO}_3)_2 \cdot 6\text{H}_2\text{O}$ (depleted uranium, R. P. Normapur, 99%) was purchased from Prolabo, and the carboxylic acids were from Aldrich. *R,S*- Me_6cyclam (meso isomer of 7(*R*),14(*S*)-5,5,7,12,12,14-hexamethyl-1,4,8,11-tetraazacyclotetradecane) was prepared as described in the literature,²⁷ and $[\text{Ni}(\text{cyclam})(\text{NO}_3)_2]$ as described in previous work.²¹ Elemental analyses were performed by MEDAC Ltd. at Chobham, UK. For all syntheses of uranyl ion complexes, the mixtures in demineralized water/organic solvent were placed in 10 mL tightly closed glass vessels and heated at 140 °C under autogenous pressure.

[Cu(R,S-Me₆cyclam)(NO₃)₂] diastereoisomers. A solution of $\text{Cu}(\text{NO}_3)_2 \cdot 3\text{H}_2\text{O}$ (0.48 g, 2.0 mmol) in methanol (5 mL) was added to a stirred solution of *R,S*- Me_6cyclam (0.58 g, 2.03 mmol) in methanol (5 mL), the initially partly gelatinous precipitate rapidly transforming into a partly soluble, violet, crystalline solid. Precipitation was improved by the addition of diethylether (30 mL) to give 0.57 g of violet crystals of $\text{N}(\text{R,S,R,S})\text{-}[\text{Cu}(\text{R,S-Me}_6\text{cyclam})(\text{NO}_3)_2]$ (61% yield) but the filtrate retained quite a deep blue-violet colour and the additional 30 mL of diethylether used to wash the crystals on the filter did not seem to cause further deposition, nor did addition of dichloromethane (50 mL). Evaporation of this filtrate/wash to dryness gave a blue residue which dissolved readily in water to provide large blue crystals of $\text{N}(\text{R,R,R,R};\text{S,S,S,S})\text{-}[\text{Cu}(\text{R,S-Me}_6\text{cyclam})(\text{NO}_3)_2]$ (0.27 g, 35% yield) on evaporation at room temperature. The identification of the diastereoisomers was based on that of the analogous perchlorates²⁸ and confirmed for the $\text{N}(\text{R,S,R,S})$ isomer by the present structural work.

[PPh₄][UO₂(C6)(NO₃)] (1). H₂C6 (15 mg, 0.10 mmol), UO₂(NO₃)₂·6H₂O (35 mg, 0.07 mmol), and PPh₄Br (42 mg, 0.10 mmol) were dissolved in water (0.5 mL). Crystals of complex **1** were obtained within one week (36 mg, 63% yield based on U). Anal. Calcd for C₃₀H₂₈NO₉PU: C, 44.18; H, 3.46; N, 1.72. Found: C, 43.95; H, 3.36; N, 1.79%.

[PPh₄][UO₂(C8)(NO₃)] (2). H₂C8 (18 mg, 0.10 mmol), UO₂(NO₃)₂·6H₂O (35 mg, 0.07 mmol), and PPh₄Br (42 mg, 0.10 mmol) were dissolved in water (0.5 mL). Only a few crystals of complex **2** were obtained within two weeks, and the yield could not be determined.

[PPh₃Me][UO₂(C7)(HC7)] (3). H₂C7 (16 mg, 0.10 mmol), UO₂(NO₃)₂·6H₂O (35 mg, 0.07 mmol), and PPh₃MeBr (36 mg, 0.10 mmol) were dissolved in water (0.7 mL) and DMF (0.2 mL). Crystals of complex **3** were obtained within two months (13 mg, 30% yield based on the acid). Anal. Calcd for C₃₃H₃₉O₁₀PU: C, 45.84; H, 4.55; N. Found: C, 45.55; H, 4.25%.

[PPh₄][H₂NMe₂][(UO₂)₂(C7)₃] (4). H₂C7 (16 mg, 0.10 mmol), UO₂(NO₃)₂·6H₂O (35 mg, 0.07 mmol), and PPh₄Br (42 mg, 0.10 mmol) were dissolved in water (0.5 mL) and DMF (0.2 mL). Crystals of complex **4** were obtained within one week (23 mg, 49% yield based on the acid). Anal. Calcd for C₄₇H₅₈NO₁₆PU₂: C, 40.32; H, 4.18; N, 1.00. Found: C, 40.25; H, 4.11; N, 1.04%.

[PPh₃Me]₂[(UO₂)₂(C8)₃] (5). H₂C8 (18 mg, 0.10 mmol), UO₂(NO₃)₂·6H₂O (35 mg, 0.07 mmol), and PPh₃MeBr (36 mg, 0.10 mmol) were dissolved in water (0.8 mL) and DMF (0.2 mL). Crystals of complex **5** were obtained within two months (32 mg, 60% yield based on the acid). Anal. Calcd for C₆₂H₇₂O₁₆P₂U₂: C, 46.22; H, 4.50. Found: C, 46.11; H, 4.42%.

[PPh₃Me]₂[(UO₂)₂(C9)₃]·2H₂O (6). H₂C9 (19 mg, 0.10 mmol), UO₂(NO₃)₂·6H₂O (35 mg, 0.07 mmol), and PPh₃MeBr (36 mg, 0.10 mmol) were dissolved in water (0.6 mL) and DMF (0.2 mL). Crystals of complex **6** were obtained within one month (24 mg, 43% yield based on the acid). Anal. Calcd for C₆₅H₈₂O₁₈P₂U₂: C, 46.22; H, 4.89. Found: C, 46.31; H, 4.65%.

$[\text{Cu}(\text{R,S-Me}_6\text{cyclam})][(\text{UO}_2)_2(\text{C7})_2(\text{C}_2\text{O}_4)] \cdot 4\text{H}_2\text{O}$ (**7**). $\text{H}_2\text{C7}$ (16 mg, 0.10 mmol), $\text{UO}_2(\text{NO}_3)_2 \cdot 6\text{H}_2\text{O}$ (35 mg, 0.07 mmol), and $\text{N}(\text{R,S,R,S})\text{-}[\text{Cu}(\text{R,S-Me}_6\text{cyclam})(\text{NO}_3)_2]$ (24 mg, 0.05 mmol) were dissolved in water (0.8 mL) and acetonitrile (0.2 mL). Crystals of complex **7** were obtained within one week (16 mg, 34% yield based on U). Anal. Calcd for $\text{C}_{32}\text{H}_{64}\text{CuN}_4\text{O}_{20}\text{U}_2$: C, 28.17; H, 4.73; N, 4.11. Found: C, 28.03; H, 4.47; N, 4.10%.

$[(\text{UO}_2)_2(\text{C7})_2(\text{HC7})_2\text{Ni}(\text{cyclam})] \cdot 2\text{H}_2\text{O}$ (**8**). $\text{H}_2\text{C7}$ (16 mg, 0.10 mmol), $\text{UO}_2(\text{NO}_3)_2 \cdot 6\text{H}_2\text{O}$ (35 mg, 0.07 mmol), and $[\text{Ni}(\text{cyclam})(\text{NO}_3)_2]$ (20 mg, 0.05 mmol) were dissolved in water (0.4 mL). Only a few crystals of complex **8** were obtained within two weeks, and the yield could not be determined.

$[(\text{UO}_2)_2\text{K}_2(\text{C7})_3(\text{H}_2\text{O})] \cdot 0.5\text{H}_2\text{O}$ (**9**). $\text{H}_2\text{C7}$ (16 mg, 0.10 mmol), $\text{UO}_2(\text{NO}_3)_2 \cdot 6\text{H}_2\text{O}$ (35 mg, 0.07 mmol), and KNO_3 (10 mg, 0.10 mmol) were dissolved in water (0.6 mL) and acetonitrile (0.2 mL). Crystals of complex **9** were obtained overnight (10 mg, 27% yield based on the acid). Anal. Calcd for $\text{C}_{21}\text{H}_{33}\text{K}_2\text{O}_{17.5}\text{U}_2$: C, 22.53; H, 2.97. Found: C, 23.17; H, 2.84%.

Crystallography. The data were collected on a Nonius Kappa-CCD area detector diffractometer²⁹ using graphite-monochromated Mo $\text{K}\alpha$ radiation ($\lambda = 0.71073 \text{ \AA}$). The crystals were introduced into glass capillaries with a protective coating of Paratone-N oil (Hampton Research). The unit cell parameters were determined from ten frames, then refined on all data. The data (combinations of φ - and ω -scans with a minimum redundancy of 4 for 90% of the reflections) were processed with HKL2000.³⁰ Absorption effects were corrected empirically with the program SCALEPACK.³⁰ The structures were solved by intrinsic phasing with SHELXT,³¹ expanded by subsequent difference Fourier synthesis and refined by full-matrix least-squares on F^2 with SHELXL-2014.³² All non-hydrogen atoms were refined with anisotropic displacement parameters. The hydrogen atoms bound to oxygen and nitrogen atoms were retrieved from difference Fourier maps when possible (see details below), and the carbon-

bound hydrogen atoms were introduced at calculated positions. All hydrogen atoms were treated as riding atoms with an isotropic displacement parameter equal to 1.2 times that of the parent atom (1.5 for CH₃, with optimized geometry). Crystal data and structure refinement parameters are given in Table 1. The molecular plots were drawn with ORTEP-3,³³ and the polyhedral representations with VESTA.³⁴ The topological analyses were conducted with TOPOS.³⁵ Special details, when present, are as follows.

Complex 4. The aliphatic chains are partly disordered over two positions which were refined with occupancy parameters constrained to sum to unity and restraints for bond lengths and angles.

Complex 6. Extensive disorder affects two aliphatic chains. One of them, disordered over two positions related by symmetry, was refined as a complete molecule with 0.5 occupancy, and two atoms of the other were refined over two positions with occupancy parameters constrained to sum to unity. Many restraints on bond lengths and displacement parameters had to be applied, and a damping factor was used in the refinement due to the instability of atoms O3 to O6, located very near their images by symmetry due to disorder. The solvent water molecule is disordered over two positions and its hydrogen atoms were not found. Twinning was detected with TwinRotMat (PLATON³⁶), and was taken into account during the refinement.

Complex 7. The highest residual electron density peaks are located near uranium atoms, probably as a result of imperfect absorption corrections.

Complex 8. Two atoms of one aliphatic chain are disordered over two positions which were refined with occupancy parameters constrained to sum to unity. Restraints on bond lengths, angles and/or displacement parameters were applied for atoms in the disordered part, and also in the cyclam molecule which is probably affected by unresolved disorder. The highest residual electron density peaks are located near the disordered chain.

Complex 9. The solvent water molecule was given half-occupancy in order to retain an acceptable displacement parameter, and its hydrogen atoms were not found. The value of the refined Flack parameter was $-0.006(11)$.

Table 1. Crystal Data and Structure Refinement Details

	1	2	3	4	5
chemical formula	C ₃₀ H ₂₈ NO ₉ PU	C ₃₂ H ₃₂ NO ₉ PU	C ₃₃ H ₃₉ O ₁₀ PU	C ₄₇ H ₅₈ NO ₁₆ PU ₂	C ₆₂ H ₇₂ O ₁₆ P ₂ U ₂
<i>M</i> (g mol ⁻¹)	815.53	843.58	864.64	1399.97	1611.19
cryst syst	monoclinic	monoclinic	monoclinic	orthorhombic	monoclinic
space group	<i>P</i> 2 ₁ / <i>c</i>	<i>P</i> 2 ₁ / <i>n</i>	<i>P</i> 2 ₁ / <i>c</i>	<i>Pcca</i>	<i>P</i> 2 ₁ / <i>c</i>
<i>a</i> (Å)	15.0644(4)	9.2845(3)	14.1580(5)	29.4157(8)	9.4938(2)
<i>b</i> (Å)	14.7060(4)	27.5528(13)	15.2308(5)	11.6583(3)	14.6791(4)
<i>c</i> (Å)	14.2217(4)	13.0534(7)	14.9688(3)	14.3357(2)	21.9542(7)
α (deg)	90	90	90	90	90
β (deg)	104.4913(17)	110.848(3)	90.051(2)	90	100.437(2)
γ (deg)	90	90	90	90	90
<i>V</i> (Å ³)	3050.40(15)	3120.6(3)	3227.84(17)	4916.2(2)	3008.93(14)
<i>Z</i>	4	4	4	4	2
<i>T</i> (K)	100(2)	100(2)	100(2)	100(2)	100(2)
reflns collcd	96650	69451	84565	65010	140334
indep reflns	5758	5884	6119	4656	5706
obsd reflns [<i>I</i> > 2 σ (<i>I</i>)]	5250	4741	5584	4122	5208
<i>R</i> _{int}	0.029	0.056	0.030	0.020	0.029
params refined	379	397	407	343	371
<i>R</i> ₁	0.024	0.029	0.021	0.027	0.021
<i>wR</i> ₂	0.062	0.063	0.052	0.068	0.052
<i>S</i>	1.043	0.973	1.033	1.072	1.051
$\Delta\rho_{\min}$ (e Å ⁻³)	-1.42	-1.14	-0.95	-1.19	-1.08
$\Delta\rho_{\max}$ (e Å ⁻³)	0.53	1.67	1.02	0.97	1.65

	6	7	8	9
chemical formula	C ₆₅ H ₅₂ O ₁₈ P ₂ U ₂	C ₃₂ H ₆₄ CuN ₄ O ₂₀ U ₂	C ₃₈ H ₇₀ N ₄ NiO ₂₂ U ₂	C ₂₁ H ₃₃ K ₂ O _{17.5} U ₂
<i>M</i> (g mol ⁻¹)	1689.30	1364.47	1469.75	1119.73
cryst syst	monoclinic	triclinic	triclinic	orthorhombic
space group	<i>C</i> 2/ <i>c</i>	<i>P</i> $\bar{1}$	<i>P</i> $\bar{1}$	<i>P</i> 2 ₁ 2 ₁ 2 ₁
<i>a</i> (Å)	16.3553(10)	11.6530(7)	10.3680(5)	9.5448(4)
<i>b</i> (Å)	22.4056(16)	14.6666(8)	11.0593(6)	17.5103(8)
<i>c</i> (Å)	18.3831(16)	19.1956(8)	12.4935(4)	19.6040(10)
α (deg)	90	88.220(3)	64.222(3)	90
β (deg)	100.475(5)	83.038(3)	84.722(3)	90
γ (deg)	90	85.811(2)	72.292(2)	90
<i>V</i> (Å ³)	6624.2(9)	3247.0(3)	1227.51(10)	3276.5(3)
<i>Z</i>	4	3	1	4
<i>T</i> (K)	100(2)	100(2)	150(2)	100(2)
reflns collcd	139310	173420	66617	73671
indep reflns	6271	12308	4660	6214
obsd reflns [<i>I</i> > 2 σ (<i>I</i>)]	4638	10379	4419	5633
<i>R</i> _{int}	0.063	0.053	0.047	0.027
params refined	465	808	323	389
<i>R</i> ₁	0.058	0.042	0.029	0.031
<i>wR</i> ₂	0.128	0.096	0.074	0.085
<i>S</i>	1.152	1.112	1.212	1.025
$\Delta\rho_{\min}$ (e Å ⁻³)	-1.75	-3.06	-2.31	-1.58
$\Delta\rho_{\max}$ (e Å ⁻³)	1.16	5.39	2.47	1.05

Luminescence Measurements. Emission spectra were recorded on solid samples using a Horiba-Jobin-Yvon IBH FL-322 Fluorolog 3 spectrometer equipped with a 450 W xenon arc

lamp, double-grating excitation and emission monochromator (2.1 nm mm⁻¹ of dispersion; 1200 grooves mm⁻¹) and a TBX-04 single photon-counting detector. The powdered compounds were put into a quartz tube and pressed to the wall of the tube, and the measurements were performed using the right angle mode. An excitation wavelength of 420 nm, a commonly used point although only part of a broad manifold, was used in all cases and the emission was monitored between 450 and 650 nm. The quantum yield measurements were performed by using an absolute photoluminescence quantum yield spectrometer Hamamatsu Quantaurus C11347 and exciting the sample between 300 and 400 nm.

RESULTS AND DISCUSSION

Synthesis. Crystals of complexes **1–9** were grown under purely hydrothermal (**1, 2** and **8**) or solvo-hydrothermal conditions, with the organic cosolvent being *N,N*-dimethylformamide (**3–6**) or acetonitrile (**7** and **9**), at a temperature of 140 °C. Systematic attempts have been made for all possible diacid/counterion/solvent combinations, and the results reported herein correspond to the experiments which succeeded in giving single crystals of suitable quality for structure determination. The crystals obtained were deposited directly from the pressurised and heated reaction mixtures and not as a result of subsequent cooling. The uranium/ligand ratio was 7:10 in all cases, so as to favour the formation of an anionic species, and the expected ratio of 2:3 is retained in complexes **4–6** and **9**, while it becomes 1:1 in **1, 2** and **7**, and 1:2 in **3** and **8** (with one ligand monoprotonated). Apart from the countercations introduced during the synthesis, other charged moieties are present in some cases: nitrate ions are retained in **1** and **2**, H₂NMe₂⁺ cations are present in **4**, and oxalate ligands in **7**. Dimethylammonium cations result from DMF hydrolysis, as very frequently observed in solvo-hydrothermal syntheses.³⁷ In situ oxalate formation under hydrothermal conditions is also very frequent,³⁸ and some in-depth studies of the mechanisms involved in particular cases have been reported.^{39,40} In the present experiments, it was found to be present only in the product obtained from the solution to which

N(*R,S,R,S*)-[Cu(*R,S*-Me₆cyclam)(NO₃)₂] had been added and thus it may have arisen from oxidative decomposition of the macrocycle.

Crystal Structures. The two complexes [PPh₄][UO₂(C6)(NO₃)] (**1**) and [PPh₄][UO₂(C8)(NO₃)] (**2**), although not isomorphous, are very similar. In both of them, the unique uranyl ion is chelated by two carboxylate groups from two C_n²⁻ ligands and one nitrate group, the uranium atom being thus in a hexagonal bipyramidal environment (Figures 1 and 2). The U–O bond lengths are unexceptional [U–O(oxido) 1.761(2)–1.772(3) Å, U–O(carboxylate) 2.424(2)–2.455(2) Å, U–O(nitrate) 2.505(2)–2.545(3) Å, including both compounds]. Zigzag chains with the nitrate groups pointing on alternate sides are formed in both cases, directed along [0 1 0] in **1** and [3 0 1] in **2**, with distances between adjacent uranium atoms of 10.4060(3) Å in **1** and 13.7353(5) Å in **2**. The well-ordered aliphatic chains in **1** adopt a *gauche-trans-gauche* (*gtg*) conformation giving the ligand an S shape, with the two nearly parallel CH₂COO⁻ groups being separated by a central C–C bond nearly perpendicular to them, and thus being in two planes offset from one another, while the equally well-ordered chains of the nearly fully extended *tggtt* conformation in **2** are kinked so that, here also, the two nearly parallel carboxylate groups are offset with respect to one another. The anionic chains are organized into sheets, parallel to (1 0 0) in **1** and to (0 1 0) in **2**, between which the countercations are located. Similar 1D polymers have previously been found in [Ag(bipy)₂]₂[UO₂(C7)(NO₃)₂]₂,¹² while linear chains with all nitrates on the same side are present in another form of the same complex.¹⁷ Examination of short contacts with PLATON³⁶ indicates the possible presence in **1** of one parallel-displaced π -stacking interaction [centroid...centroid distance 4.20 Å, slippage 1.37 Å], and two CH... π interactions involving either an aliphatic or an aromatic proton [H...centroid distances 2.73 and 2.91 Å, C–H...centroid angles 142 and 161°]. Calculation of the Hirshfeld surfaces⁴¹ with CrystalExplorer⁴² for both the cation and the asymmetric unit of the uranyl

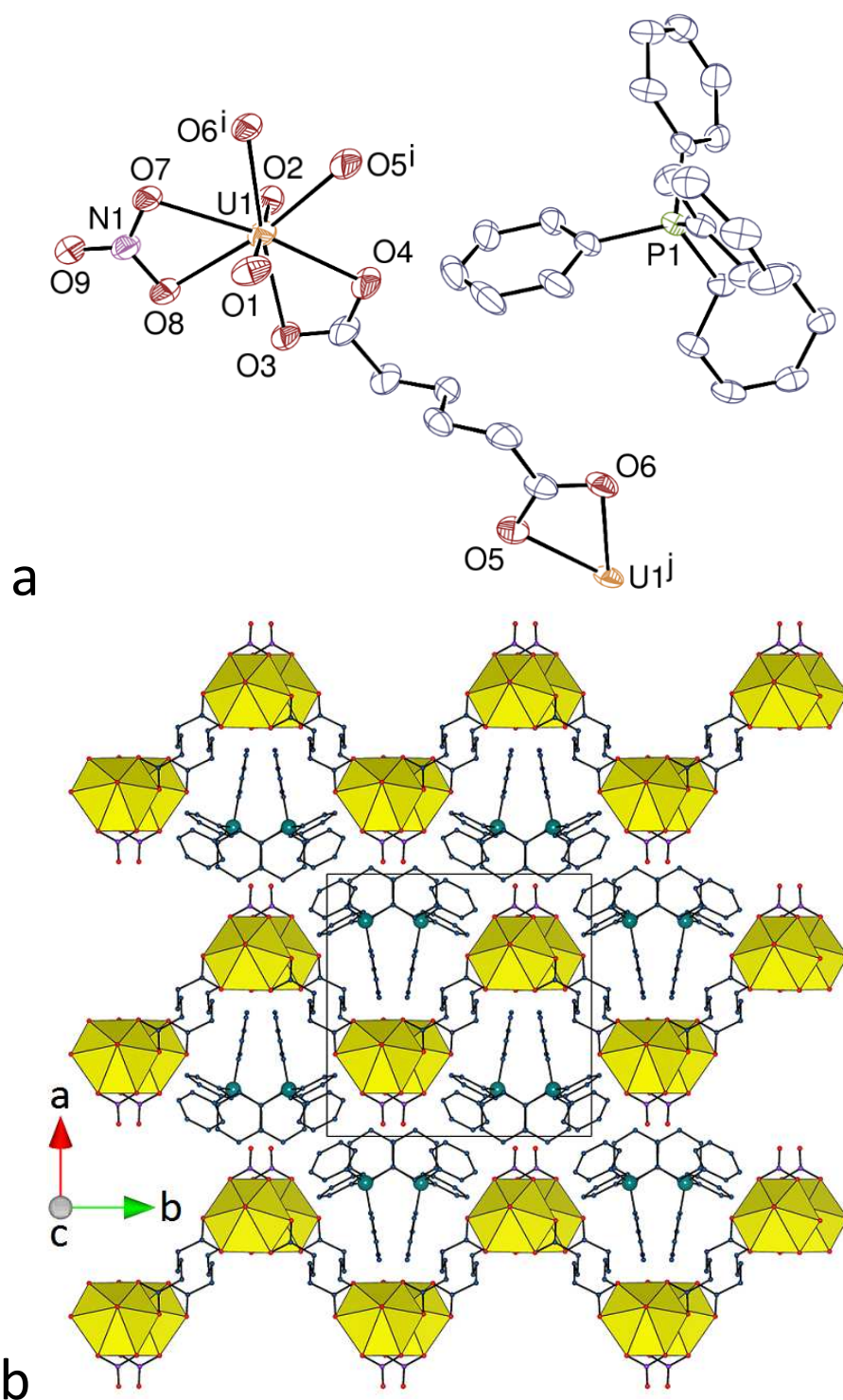


Figure 1. (a) View of compound **1**. Displacement ellipsoids are drawn at the 50% probability level. Symmetry codes: $i = 1 - x, y + 1/2, 3/2 - z$; $j = 1 - x, y - 1/2, 3/2 - z$. (b) View of the packing with uranium coordination polyhedra colored yellow. Hydrogen atoms are omitted in both views.

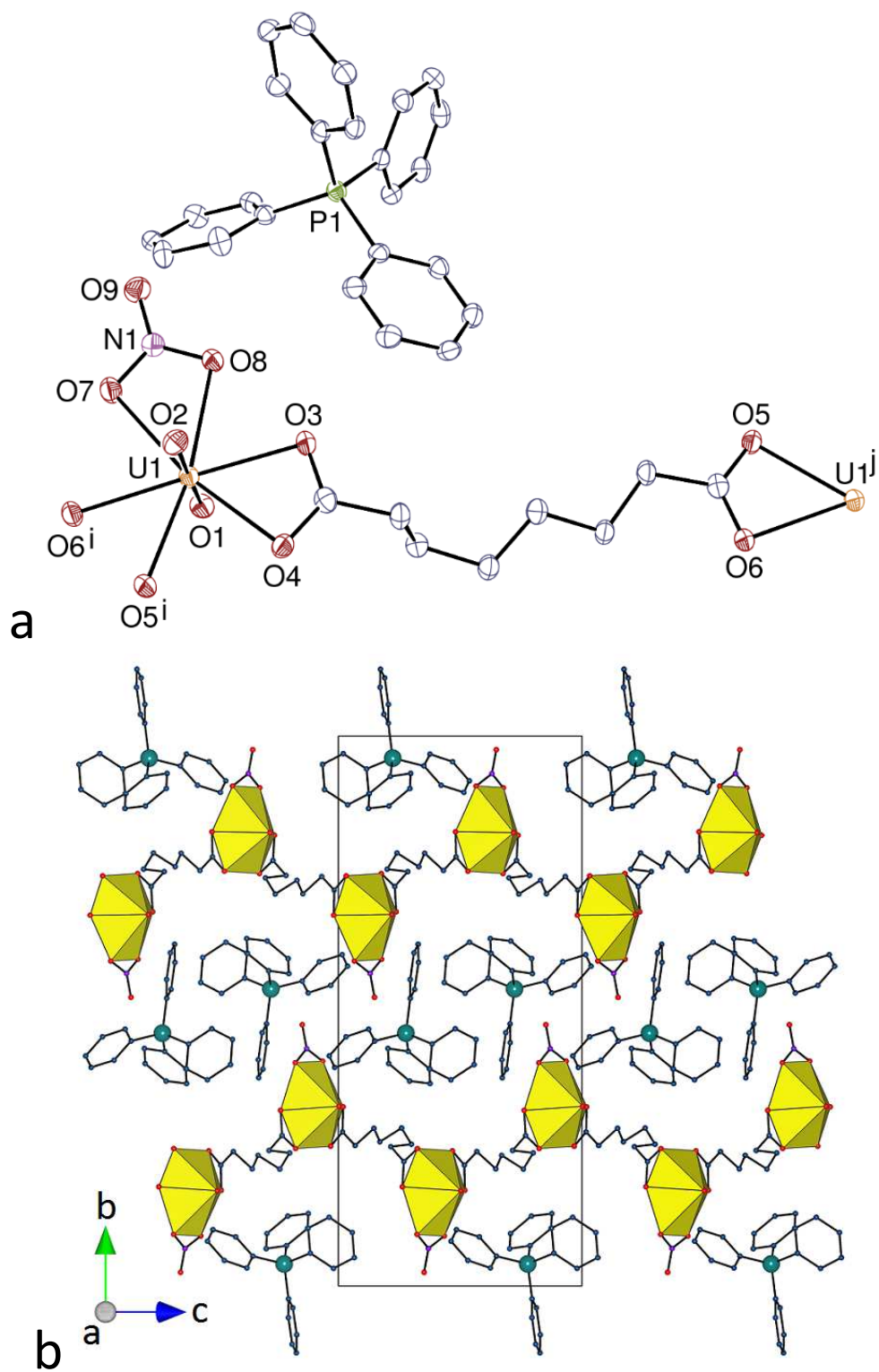


Figure 2. (a) View of compound **2**. Displacement ellipsoids are drawn at the 50% probability level. Symmetry codes: $i = x + 3/2, 1/2 - y, z + 1/2$; $j = x - 3/2, 1/2 - y, z - 1/2$. (b) View of the packing with uranium coordination polyhedra colored yellow. Hydrogen atoms are omitted in both views.

polymer provides evidence for both some CH...C(aromatic) (“CH... π ”) and more abundant CH...O hydrogen bonding^{43,44} interactions beyond dispersion. Reciprocal CH...C(aromatic) interactions between cations with a P...P separation of 6.9044(13) Å may be considered to define a cation pair involved in a “phenyl embrace”,⁴⁵ although other CH...C(aromatic) interactions also link cations into an undulating chain with P...P 7.7567(6) Å. A given cation undergoes several interactions with the anionic polymer corresponding to CH...O hydrogen bonds involving aromatic protons on all four of the phenyl groups and carboxylate or nitrate (terminal) oxygen atoms [C...O 3.202(4)–3.260(4) Å, C–H...O 138–161°]. The carboxylate atom O3 in particular is an acceptor of two such bonds from two aromatic rings in the same counterion. These interactions serve to create a 3D character to the lattice and accompany the fact that the shortest U...U separation of 7.2691(2) Å is not one between metal centres in the polymer chain but between centres in adjacent chains. The intermolecular weak interactions are not very different in compound **2**, with one possible parallel-displaced π -stacking interaction [centroid...centroid distance 4.17 Å, slippage 1.29 Å], one CH(aliphatic)... π interaction [H...centroid 2.65 Å, C–H...centroid 131°], and CH...O hydrogen bonds involving aliphatic or aromatic protons and the carboxylate, nitrate (terminal), and two uranyl oxido oxygen atoms [C...O 3.235(5)–3.410(5) Å, C–H...O 118–159°]. Here, however, only three of the four phenyl groups of the cation are involved in CH...O interactions, although they are still sufficient to create a 3D array of the lattice assisted by a phenyl embrace (involving reciprocal C...H contacts at 2.80 Å) giving cation pairs 6.551(2) Å apart. The Kitaigorodski packing index (KPI) values calculated with PLATON³⁶ are 0.67 for **1** and 0.69 for **2**, showing the absence of solvent-accessible free spaces and reflecting the extensive nature of the cation...anion interactions.

Although they were both synthesized from H₂C₇ with DMF as organic cosolvent, the two following complexes differ in their stoichiometry and in the nature of the counterions

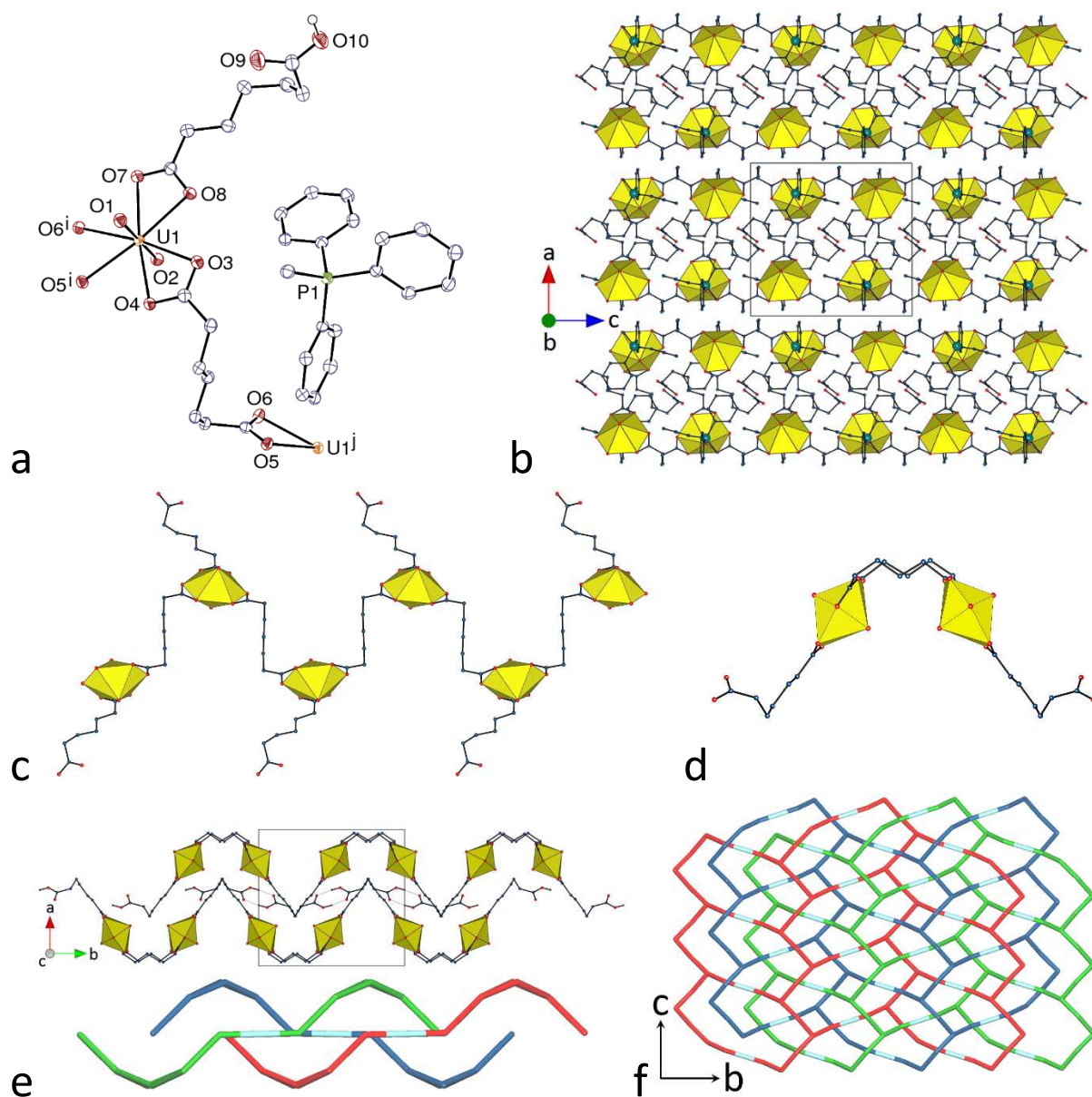


Figure 3. (a) View of compound **3**. Displacement ellipsoids are drawn at the 50% probability level. Carbon-bound hydrogen atoms are omitted. Symmetry codes: $i = x, 3/2 - y, z - 1/2$; $j = x, 3/2 - y, z + 1/2$. (b) Packing with chains viewed side-on and hydrogen atoms omitted. (c) and (d) Two views of the 1D polymer, down the a and c axes, respectively. (e) View of one three-fold interpenetrated hydrogen bonded layer with the 1D coordination polymers viewed end-on and hydrogen bonds shown as dotted lines (top), and simplified view in the same orientation with the three networks in red, blue and green and hydrogen bonds shown as pale blue rods (bottom). (f) Simplified view of the hydrogen bonded entanglement down the a axis.

present, and are shown to be $[\text{PPh}_3\text{Me}][\text{UO}_2(\text{C7})(\text{HC7})]$ (**3**) and $[\text{PPh}_4][\text{H}_2\text{NMe}_2][(\text{UO}_2)_2(\text{C7})_3]$ (**4**). One of the ligands in **3** retains one of its carboxylic protons, while dimethylammonium ions generated in situ are present in **4** (see Experimental Section). The unique uranyl cation in **3** is chelated by three carboxylate groups from two C7^{2-} and one HC7^- ligands (Figure 3), the uranium atom being thus in a hexagonal bipyramidal environment [U–O(oxido) 1.7731(19) and 1.7749(19) Å, U–O(carboxylate) 2.4397(18)–2.4992(18) Å]. The bridging dicarboxylate ligands, which assume here also an *S* shape, as for C6 in **1**, due to their *gttg* conformation, generate a 1D polymeric chain with a square wave profile directed along the *c* axis, and the mono-deprotonated ligands, with a *ttgg* conformation giving a twisted carboxylic acid group, are terminal, like the nitrate ions in **1** and **2**. The carboxylic acid groups are involved in reciprocal hydrogen bonding with their image by inversion [O10 \cdots O9^k 2.649(4) Å, O10–H \cdots O9^k 171°; symmetry code: $k = 1 - x, -y, 1 - z$], so that chains are connected to one another along the *b* axis to form layers parallel to (1 0 0). Within each of these layers, three strongly corrugated hydrogen bonded networks with hexagonal cells are interpenetrated in the parallel 2D + 2D + 2D \rightarrow 2D mode. The dicarboxylate ligands are located on the sides of the layers, while the carboxylic groups are in the middle and connect chains located alternately on either side of the layer. Sufficient voids are present in the lattice to accommodate the PPh_3Me^+ counterions, which are too distant from one another for any form of “embrace” to occur [minimum P \cdots P distance 8.9568(8) Å]; one CH(aliphatic) $\cdots\pi$ interaction [H \cdots centroid 2.93 Å, C–H \cdots centroid 135°] is present, as well as several CH \cdots O hydrogen bonds involving methyl or aromatic protons of the counterion and carboxylic/ate oxygen atoms [C \cdots O 3.166(3)–3.384(3) Å, C–H \cdots O 136–171°]. With a KPI of 0.71, the lattice contains no solvent-accessible free space, once again possibly reflecting the multiplicity of interactions occurring between the lattice components.

The unique uranyl ion in complex **4** is chelated by three carboxylate groups from three $C7^{2-}$ ligands [U–O(oxido) 1.766(3) and 1.770(3) Å, U–O(carboxylate) 2.455(3)–2.487(3) Å]. The aliphatic chains of the two pimelate ligands are partly disordered (see Experimental Section), and one of them has twofold rotation symmetry; although their conformation is masked by disorder, one appears to be a partly extended, divergent ligand disordered over *gtgt* and *ttgt* conformers, while the other, symmetric one is curved in an approximately *gggg* conformation (Figure 4). In contrast to complexes **1–3**, all the ligands here are bridging, and a ladder-like 1D polymer running along the *b* axis direction is formed, analogous to those found

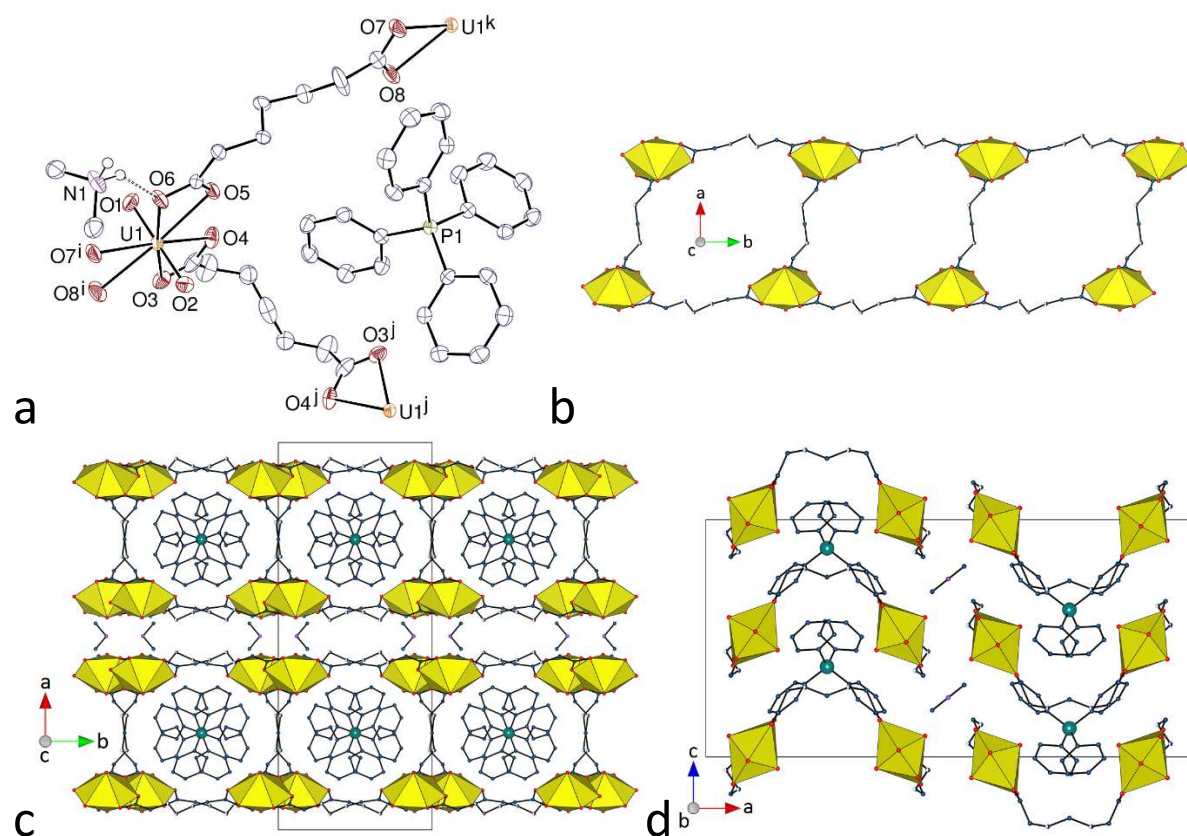


Figure 4. (a) View of compound **4**. Displacement ellipsoids are drawn at the 50% probability level. Carbon-bound hydrogen atoms are omitted and the hydrogen bond is shown as a dashed line. Symmetry codes: $i = x, y - 1, z$; $j = 3/2 - x, -y, z$; $k = x, y + 1, z$. (b) View of the 1D ladder-like chain. (c) Packing with chains viewed side-on. (d) Packing with chains viewed end-on. Only one position of the disordered atoms is shown in all views.

in $[\text{Fe}(\text{bipy})_3][(\text{UO}_2)_2(\text{C7})_3] \cdot 3\text{H}_2\text{O}$ (where the two inequivalent dicarboxylate ligands have *tttt* and *tgtg* conformations) and $[\text{Cu}(\text{bipy})_2]_2[(\text{UO}_2)_2(\text{C9})_3]$.¹⁶ However, the curved shape of the central ligands in **4** gives the polymer a gutter shape, in which part of the PPh_4^+ counterion is located. The chains are stacked so as to form layers parallel to (1 0 0), with a reverse orientation of the gutter cavity in adjacent layers. Within the layers, channels directed along the *c* axis contain the PPh_4^+ counterions, while the H_2NMe_2^+ cations, with twofold rotation symmetry, are located between the layers, which they connect to one another through hydrogen bonding to carboxylate groups [N1...O6 2.762(3) Å, N1–H...O6 144°]. A short contact between aromatic groups within the columns may indicate a possible π -stacking interaction [centroid...centroid 4.079(2) Å, dihedral angle 26.0(2)°]; one CH(aliphatic)... π interaction [H...centroid 2.89 Å, C–H...centroid 152°] and four CH...O hydrogen bonds [C...O 3.159(5)–3.344(6) Å, C–H...O 136–139°] may be present as well. Partial occupancies and disorder render CrystalExplorer inapplicable to this structure. The two cations clearly enter into competition for *O*-donor sites, though the “classical” NH...O interactions presumably are stronger than “non-classical” CH...O,^{43,44} which may explain why the PPh_4^+ cations are found in “embrace” chains [P...P 7.16785(9) Å] running parallel to the *c* axis.

Uranyl tris-chelation by carboxylate groups is also found in the complex $[\text{PPh}_3\text{Me}]_2[(\text{UO}_2)_2(\text{C8})_3]$ (**5**), shown in Figure 5. The uranium atom environment is unexceptional [U–O(oxido) 1.767(2) and 1.771(2) Å, U–O(carboxylate) 2.4547(18)–2.5080(19) Å], and one of the C8^{2-} ligands is centrosymmetric and in its fully extended *tttt* conformation, while the other is the curved *gtgtt* conformer. A 1D polymer is formed here also, but one in which doubly-bridged uranyl dimers are connected to one another by the extended, divergent ligands. A similar connectivity was previously found in a complex with C6^{2-} including diprotonated 1,2-bis(4-pyridyl)ethane,⁸ and in a complex with C10^{2-} including cucurbit[6]uril molecules.¹⁰ The chains in **5** run along either [2 1 0] or [2 $\bar{1}$ 0], alternate sheets

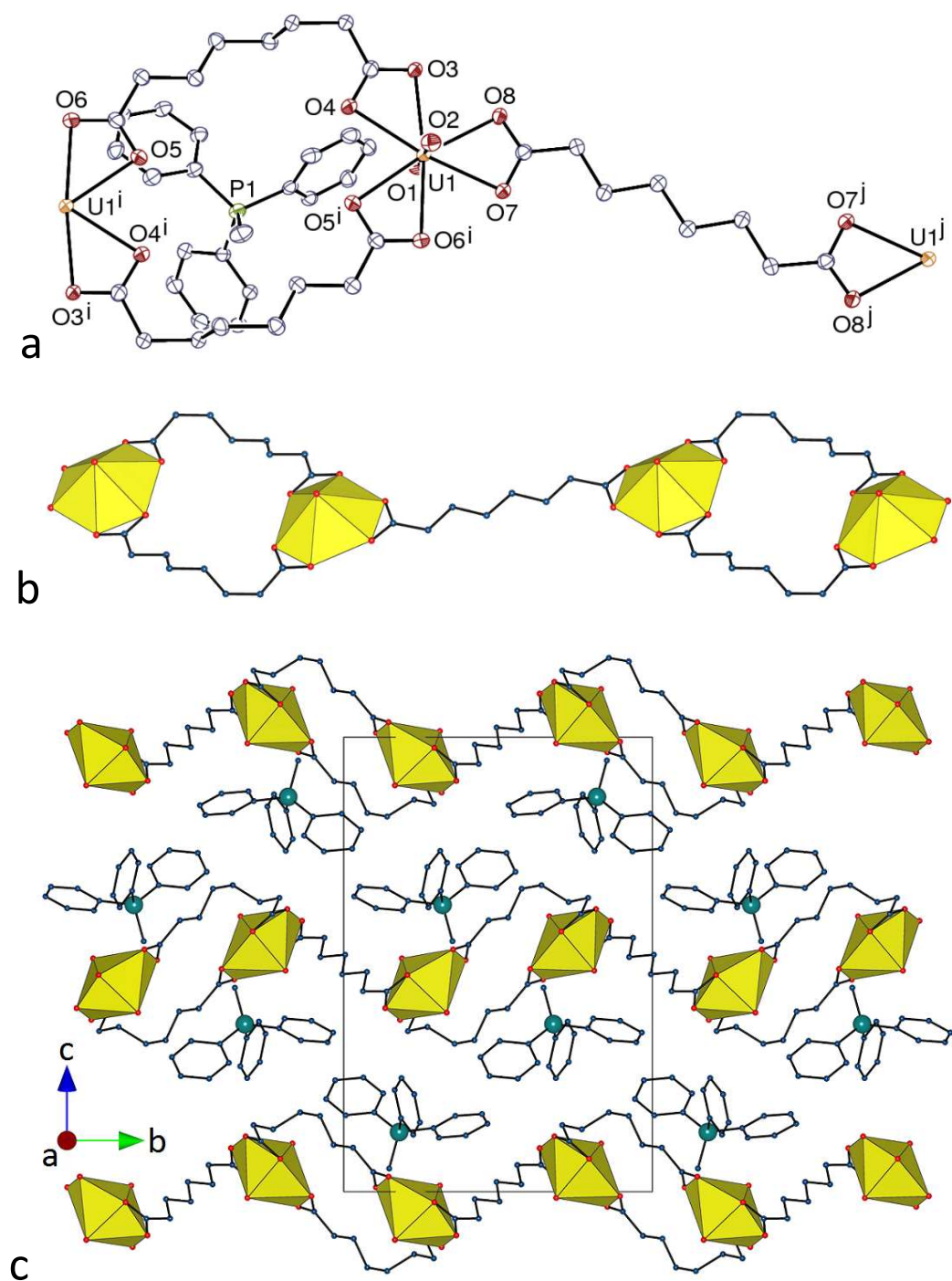


Figure 5. (a) View of compound **5**. Displacement ellipsoids are drawn at the 50% probability level. Symmetry codes: $i = 1 - x, 1 - y, 1 - z$; $j = -x - 1, 2 - y, 1 - z$. (b) View of the 1D coordination polymer. (c) View of the packing. Hydrogen atoms are omitted in all views.

of chains of either orientation parallel to (0 0 1) being separated by double layers of counterions.

No evidence of interactions indicative of cation embrace is apparent [minimum P...P distance

8.2080(15) Å], but one CH(aliphatic)⋯π interaction [H⋯centroid 2.72 Å, C–H⋯centroid 172°] and three CH⋯O hydrogen bonds [C⋯O 3.320(4)–3.430(4) Å, C–H⋯O 142–165°] characterize the interactions of the cations with the polymer, each cation having contacts to five separate uranyl coordination spheres. The KPI of 0.70 is indicative of a compact packing with no solvent-accessible free space.

Only one complex with the C9²⁻ azelate ligand has been obtained in the present work, [PPh₃Me]₂[(UO₂)₂(C9)₃]·2H₂O (**6**). Here also, the unique uranyl ion is chelated by three carboxylate groups [U–O(oxido) 1.773(4) and 1.775(4) Å, U–O(carboxylate) 2.444(11)–2.481(14) Å] (Figure 6). Two carboxylate ligands have twofold rotation symmetry and the other is disordered around a twofold rotation axis (see Experimental Section); the ligand containing O7 and O8 is in its fully extended *ttttt* conformation, that containing the disordered atoms O3 to O6, although of irregular conformation, is divergent, but the third, including O9 and O10, which, like the second, has some *gauche* links, is bent at both ends so that the two nearly parallel carboxylate groups are pointing in the same direction. These different conformations result in quite different separations between uranyl centres [15.3647(12), 11.7801(9) and 8.7447(8) Å]. In contrast to complexes **1–5**, a two-dimensional (2D) assembly parallel to (0 1 0) is formed here, which has the point (Schläfli) symbol {6³} and the honeycomb hcb topology. This geometry has previously been found with C10²⁻, C12²⁻, and C13²⁻,^{15,16} with in all cases very distorted hexagonal cells, far from planar, as could be expected for such long and flexible ligands. The present case is no exception, the layers being deeply corrugated, particularly when viewed down the [1 0 $\bar{1}$] axis, and they are associated into pairs, with slight interdigitation visible along the same axis (Figure 6c). These pairs are then stacked with, here also, slight interdigitation apparent when the packing is viewed down the *a* axis (Figure 6d) or the *c* axis. As in complex **5**, no parallel-displaced π-stacking interaction between cations is evident but

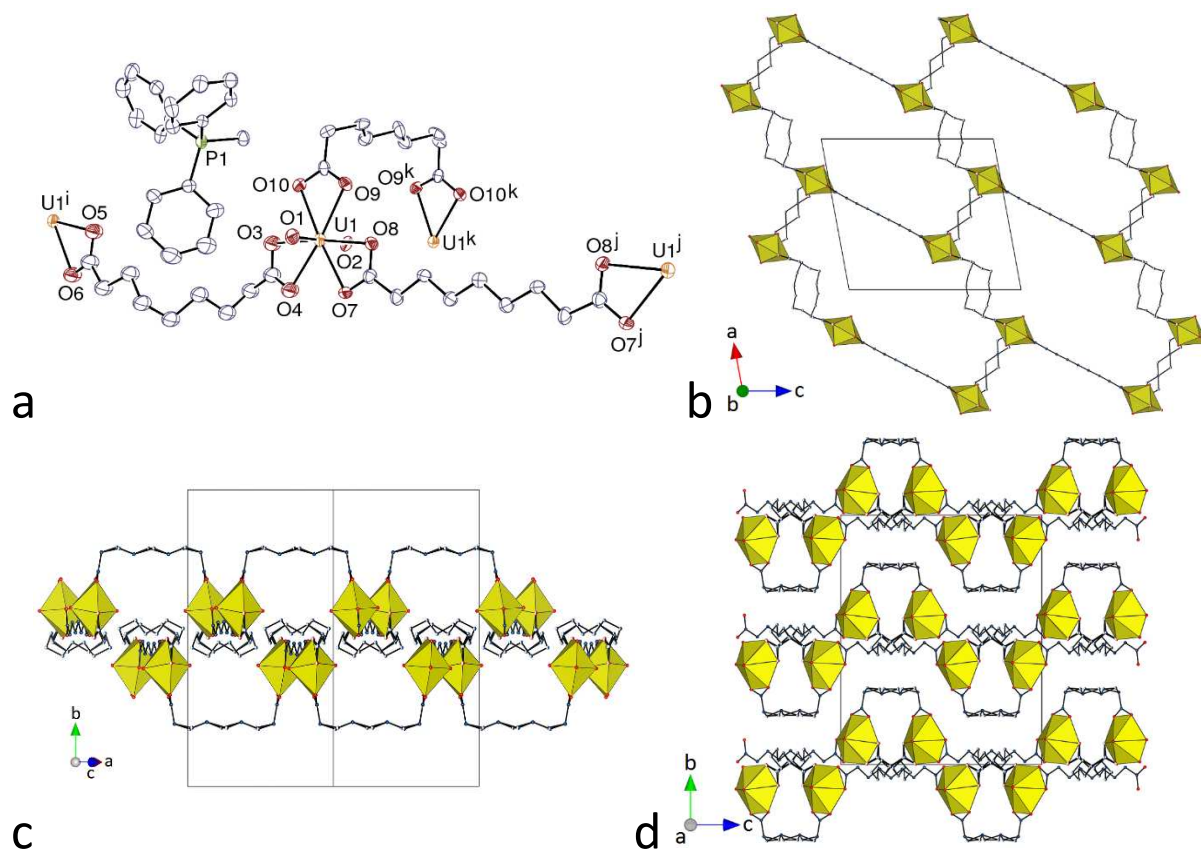


Figure 6. (a) View of compound **6**. Displacement ellipsoids are drawn at the 40% probability level. Only one position of the disordered atoms is represented. Symmetry codes: $i = 1 - x, y, 3/2 - z$; $j = 2 - x, y, 1/2 - z$; $k = 2 - x, y, 3/2 - z$. (b) View of the honeycomb 2D network. (c) Interdigitation in the bilayers. (d) Packing with layers viewed edge-on. Both positions of the disordered aliphatic chains are shown and counterions are omitted in the last three views. Solvent molecules and hydrogen atoms are omitted in all views.

here there are close centrosymmetric cation pairs [$P \cdots P$ 6.619(3) Å] involving facing triphenyl units associated with reciprocal $CH \cdots C(\text{aromatic})$ contacts of ~ 2.8 Å, and there are two possible $CH(\text{aliphatic}) \cdots \pi$ interactions [$H \cdots \text{centroid}$ 2.78 and 2.96 Å, $C-H \cdots \text{centroid}$ 147 and 166°] and several $CH \cdots O$ hydrogen bonds [$C \cdots O$ 3.076(15)–3.507(8) Å, $C-H \cdots O$ 123–159°] which result in 3D linking of the lattice components.

Two compounds including 3d-block transition metal ion complexes with macrocyclic nitrogen donors were obtained, both with the pimelate ligand. The asymmetric unit in $[Cu(R,S-$

$\text{Me}_6\text{cyclam})][(\text{UO}_2)_2(\text{C}_7)_2(\text{C}_2\text{O}_4)] \cdot 4\text{H}_2\text{O}$ (**7**) contains three uranyl ions, all chelated by two C_7^{2-} and one oxalate ligands (the latter formed in situ, see Experimental Section) [$\text{U}-\text{O}(\text{oxido})$ 1.765(5)–1.781(5) Å, $\text{U}-\text{O}(\text{carboxylate})$ 2.458(5)–2.519(5) Å], and two $[\text{Cu}(\text{R},\text{S}-\text{Me}_6\text{cyclam})]^{2+}$ cations, one of them centrosymmetric, shown thus to have the $\text{N}(\text{R},\text{S},\text{R},\text{S})$ configuration assumed for the reactant complex (Figure 7). The three independent C_7^{2-} ligands adopt irregular conformations (*tgtg* and twice *tggg*), and all are clearly divergent. A 1D ladder-like polymeric chain parallel to $[2\ 1\ \bar{1}]$ is formed, which derives from that found in complex **3** by replacement of the central, curved C_7^{2-} by a smaller and planar oxalate ligand, with the consequence that the whole assembly in **7** is also planar. The copper(II) cations are bound to the four nitrogen atoms of the macrocycle [$\text{Cu}-\text{N}$ 2.009(6)–2.039(6) Å], and, forming no contact with oxygen atoms of the polymer shorter than ~ 3.5 Å, they are considered as isolated counterions except for their hydrogen bonding interactions (see ahead). When viewed down the chain axis, the packing displays layers containing alternate cations and anions, these layers being offset in bump-to-hollow fashion with respect to one another. The presence of the macrocyclic secondary amines and the lattice water molecules results in the formation of numerous hydrogen bonds with, among others, carboxylate groups as acceptors. The $[\text{Cu}(\text{R},\text{S}-\text{Me}_6\text{cyclam})]^{2+}$ moieties are hydrogen bonded to quartets of lattice water molecules only [$\text{N}\cdots\text{O}$ 2.880(8)–2.972(7) Å, $\text{N}-\text{H}\cdots\text{O}$ 151–176°], these quartets being hydrogen bonded units within themselves but also providing further hydrogen bonding connection to the anionic polymer, all $\text{OH}\cdots\text{O}$ and $\text{NH}\cdots\text{O}$ hydrogen bonds being located within the layers. The C_7^{2-} ligands on both edges of the ribbon-like chains are involved in $\text{CH}\cdots\text{O}$ hydrogen bonds with uranyl oxido and carboxylato oxygen atoms pertaining to adjacent layers, thus uniting them into a 3D network. The packing has a KPI of 0.71, indicating that no extra free space is present.

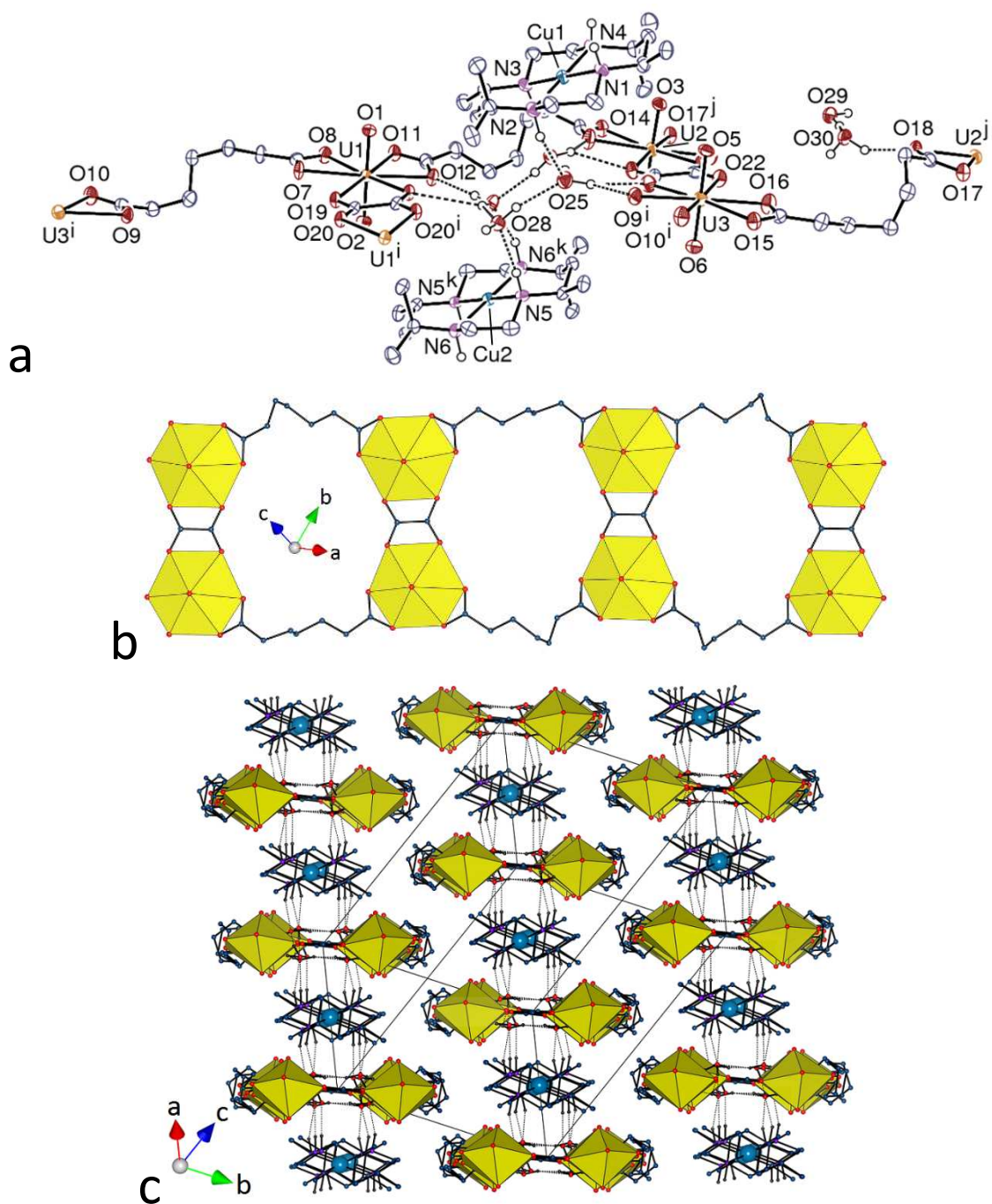


Figure 7. (a) View of compound 7. Displacement ellipsoids are drawn at the 50% probability level. Carbon-bound hydrogen atoms are omitted and the hydrogen bonds are shown as dashed lines. Symmetry codes: $i = -x, 1 - y, 1 - z$; $j = 2 - x, 2 - y, -z$; $k = 1 - x, 1 - y, 1 - z$. (b) View of the 1D ladder-like chain. (c) Packing with chains viewed end-on; solvent molecules and carbon-bound hydrogen atoms are omitted, and hydrogen bonds are shown as dotted lines.

The second compound including a 3d-block cation complex is $[(\text{UO}_2)_2(\text{C7})_2(\text{HC7})_2\text{Ni}(\text{cyclam})]\cdot 2\text{H}_2\text{O}$ (**8**), which involves a less bulky macrocycle and a metal ion, Ni^{II} , with significantly different coordinative properties to Cu^{II} . The unique uranyl cation is chelated by one carboxylate group and bound to three more oxygen atoms from bridging carboxylate groups in three different ligands [U–O(oxido) 1.767(4) and 1.770(3) Å, U–O(carboxylate) 2.435(4) and 2.500(4) Å for the chelating group, and 2.315(4)–2.371(3) Å for the bridging groups]. The nickel(II) cation, located on an inversion centre, is bound to the four nitrogen atoms of cyclam [Ni–N 2.054(4) and 2.066(4) Å], and, in contrast to copper(II) in **7**, it is also axially bound to two carboxylate oxygen atoms, at 2.144(3) Å (Figure 8). The

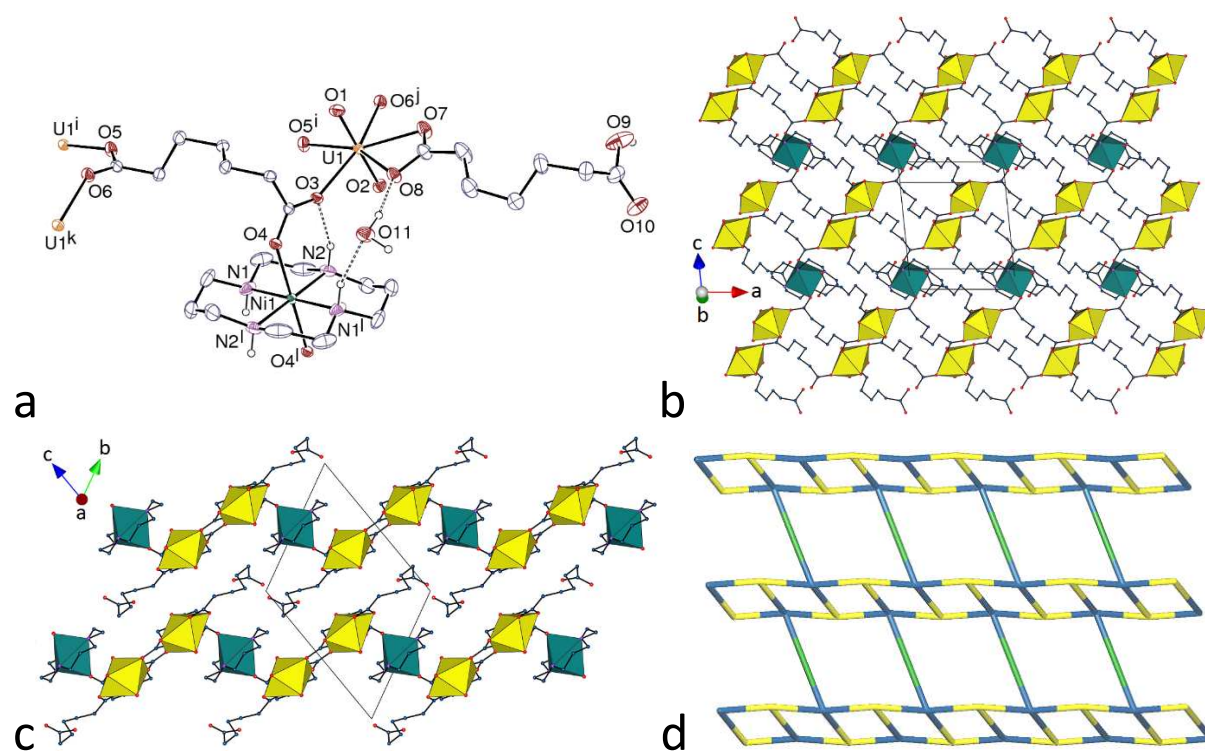


Figure 8. (a) View of compound **8**. Displacement ellipsoids are drawn at the 30% probability level. Carbon-bound hydrogen atoms are omitted and the hydrogen bonds are shown as dashed lines. Symmetry codes: $i = 2 - x, 2 - y, 1 - z$; $j = x - 1, y, z$; $k = x + 1, y, z$; $l = 2 - x, 1 - y, 2 - z$. (b) View of the 2D network with uranium coordination polyhedra colored yellow and those of nickel(II) green. (c) Packing with layers viewed edge-on. Only one position of the disordered atoms is represented in all three views. (d) Simplified view of the 2D network (yellow, uranium nodes; green, nickel(II) links; blue, ligand nodes); same orientation as in (b).

dicarboxylate ligand is bridging bidentate at both ends, while the singly deprotonated one, which is partly disordered, is chelating through the carboxylate group, the carboxylic group being uncoordinated as in complex **3**. Both ligands have irregular conformations, the fully deprotonated one being the *gtgt* conformer which is essentially a divergent connector. Disorder in the HC7^- ligands appears to involve the *tgtg* and *tggt* conformers. Planar ribbon-like chains running along the *a* axis are formed, which contain doubly bridged uranyl dimers and pendent carboxylic acid groups on both edges. These ribbons are further connected to one another by the $\text{Ni}(\text{cyclam})^{2+}$ moieties so as to form a 2D assembly parallel to (0 1 1), the ribbons being tilted with respect to the layer plane. The network is binodal (dicarboxylate ligand and uranyl cations), the nickel(II) cations being simple links, and it has the point symbol $\{4^2.6^3.8\}\{4^2.6\}$ and the V_2O_5 topological type. Due to the tilting of the ribbons within the layers, the carboxylic groups are directed toward the interlayer space; however, those pertaining to different layers do not face exactly each other so as to form double hydrogen bonds as in **3**, but each of them is bound instead to a lattice water molecule which is itself linked to one carboxylate oxygen atom and to a carboxylic group of the adjacent layer (Figure 9), thus forming a water-mediated 3D

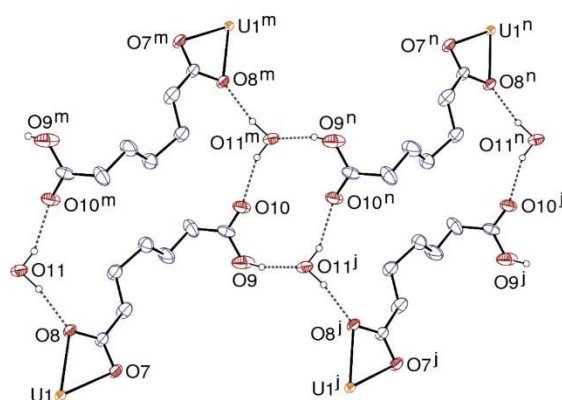


Figure 9. Hydrogen bonding network involving HC7^- ligands and water molecules in compound **8**. Carbon-bound hydrogen atoms are omitted and the hydrogen bonds are shown as dashed lines. Symmetry codes: $j = x - 1, y, z$; $m = 1 - x, -y, 2 - z$; $n = -x, -y, 2 - z$.

network. The carboxylic groups and water molecules form a ring corresponding to the graph set descriptor^{46,47} $R_4^4(12)$, while larger $R_4^4(24)$ rings are built by two water molecules and two HC7⁻ ligands. The amine atom N2 is hydrogen bonded to the bridging carboxylate atom O3 [N2...O3 2.917(6) Å, N2-H...O3 152°], a feature previously found in other carboxylate complexes including this counterion,²¹ and the other amine group is bound to the lattice water molecule.

The last compound in the present series, [(UO₂)₂K₂(C7)₃(H₂O)]·0.5H₂O (**9**), contains a counterion quite different from those in complexes **1–8**, since it is a single alkali metal cation. Although uranyl ion complexes with C_n²⁻ dicarboxylate ligands incorporating alkali or alkaline-earth metal cations have been reported for $n = 4$ (succinate),⁴⁸ and $n = 5$ (glutarate),^{49–52} for example (with formation of hydrogen bonded interpenetrated frameworks in one case⁵⁰), no example has been reported with larger n values. The asymmetric unit in **9**, which crystallizes in the Sohncke group $P2_12_12_1$, contains two uranyl cations, both chelated by three carboxylate groups [U–O(oxido) 1.763(8)–1.774(9) Å, U–O(carboxylate) 2.443(7)–2.508(7) Å], and two potassium cations in different environments (Figure 10). Atom K1 is bound to six carboxylate oxygen atoms from six different ligands [K–O 2.673(8)–2.738(8) Å], its environment being of irregular geometry, and atom K2 is bound to six carboxylate oxygen atoms [K–O 2.677(9)–3.095(8) Å] and one water molecule [2.690(10) Å]. K2 is also possibly bound to the uranyl oxido atom O3, with a distance of 3.462(9) Å which is longer than the usual values of ~2.6–2.8 Å;²² however, this interaction appears to be significant from examination of the Hirshfeld surface of the potassium cation. The three inequivalent dicarboxylate ligands present adopt *ttg*, *tggt* and *gttg* conformations, linking uranyl ion centres with U...U separations of 10.8006(7), 10.8374(6) and 9.5448(4) Å, respectively. All three ligands are identically coordinated through their two carboxylate groups, being chelating toward uranium and bridging toward two potassium cations, the common coordination mode being thus $\mu_3\text{-}\kappa^1\text{O}:\kappa^2\text{O},\text{O}':\kappa^1\text{O}'$. Each UO₆

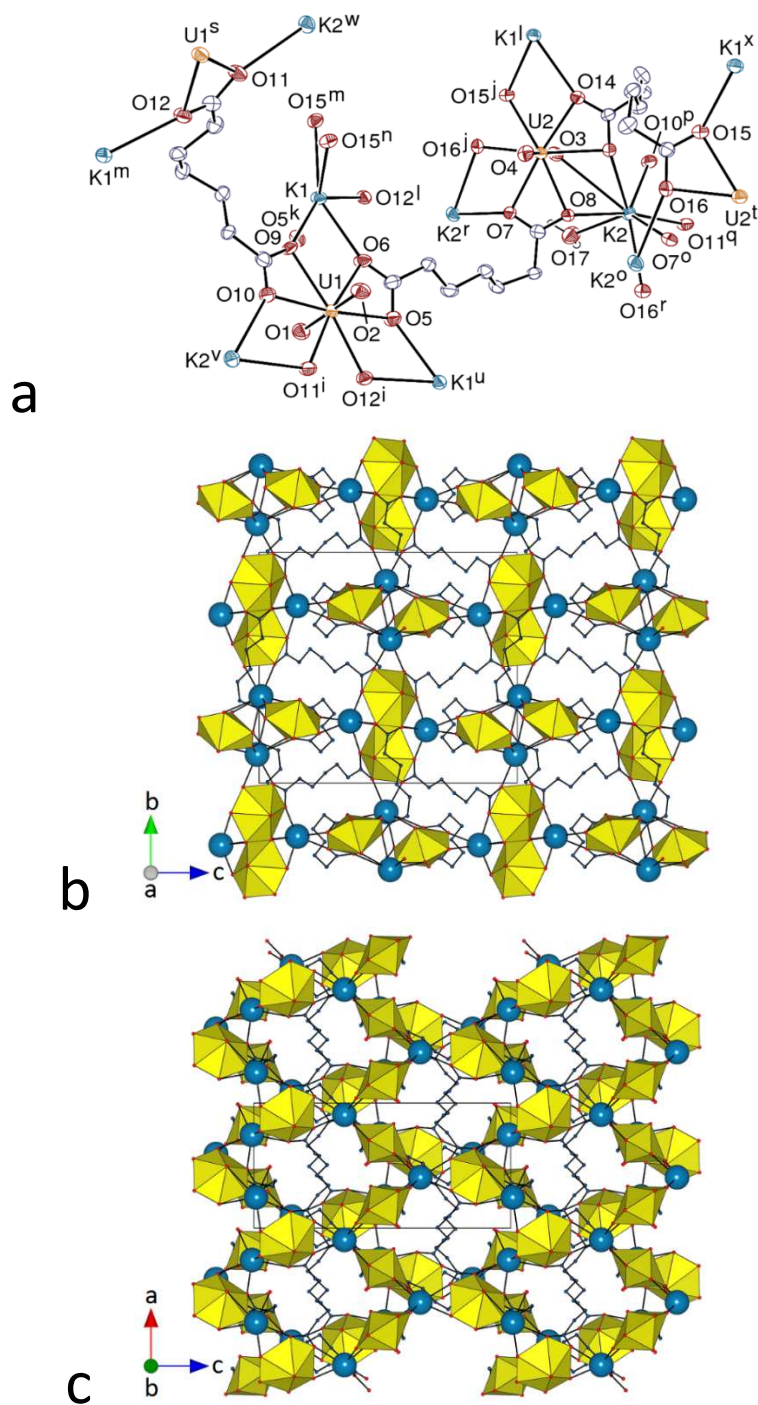


Figure 10. (a) View of compound **9**. Displacement ellipsoids are drawn at the 40% probability level. Symmetry codes: $i = 3/2 - x, -y, z - 1/2$; $j = x - 1, y, z$; $k = x - 1/2, 1/2 - y, 1 - z$; $l = 1 - x, y + 1/2, 3/2 - z$; $m = 1 - x, y - 1/2, 3/2 - z$; $n = 2 - x, y - 1/2, 3/2 - z$; $o = x + 1/2, 3/2 - y, 1 - z$; $p = x, y + 1, z$; $q = 3/2 - x, 1 - y, z - 1/2$; $r = x - 1/2, 3/2 - y, 1 - z$; $s = 3/2 - x, -y, z + 1/2$; $t = x + 1, y, z$; $u = x + 1/2, 1/2 - y, 1 - z$; $v = x, y - 1, z$; $w = 3/2 - x, 1 - y, z + 1/2$; $x = 2 - x, y + 1/2, 3/2 - z$. (b) and (c) Two views of the 3D framework with uranium coordination polyhedra colored yellow and potassium atoms shown as blue spheres. Solvent molecules and hydrogen atoms are omitted in all views.

planar array is thus connected to three potassium cations, thus making a tetranuclear, trigonal building unit. The UO_6K_3 unit is nearly planar in the case of U1 (root mean square (rms) deviation 0.13 Å), but, in the case of U2, the potassium cation K2 involved in oxido bonding is displaced by 2.076(8) Å from the plane defined by the other 9 atoms (rms 0.30 Å). Overall, the coordination polymer formed is 3D, but it is worth examining the assembly formed by uranyl ions and dicarboxylate ligands alone. The latter is a uninodal 2D network parallel to (0 1 0) and with the point symbol $\{8^2.10\}$, similar to that found in $[\text{NH}_4]_2[(\text{UO}_2)_2(\text{C7})_3]\cdot 2\text{H}_2\text{O}$, which crystallizes in the same space group as **9**, and with quite similar unit cell parameters.¹² These networks are very convoluted, being built of central chains running parallel to one another and surrounded on either side by two sets of chains running in the transverse direction (Figure 11). In both compounds, each network is entangled with its two neighbours along the *b* axis, resulting in 2D \rightarrow 3D parallel polycatenation. Uranyl and C7^{2-} ligands are thus sufficient for framework formation, and K^+ cations are further linkers between the individual 2D subunits, a role analogous to that of the ammonium cations in the former compound, which are hydrogen bonded to carboxylate oxygen atoms; this may be viewed as a consequence of the “pseudometal” behaviour of NH_4^+ , with properties akin to those of K^+ ,⁵³ as previously noted in the case of other uranyl carboxylate complexes.⁵⁴ It is notable that the thick layers, with significant extension in the third dimension, found in **9** give rise to polycatenation, while the flatter hydrogen bonded layers in **3** result in interpenetration only (with no increase in dimensionality). With a KPI of 0.75, the framework has no significant free space.

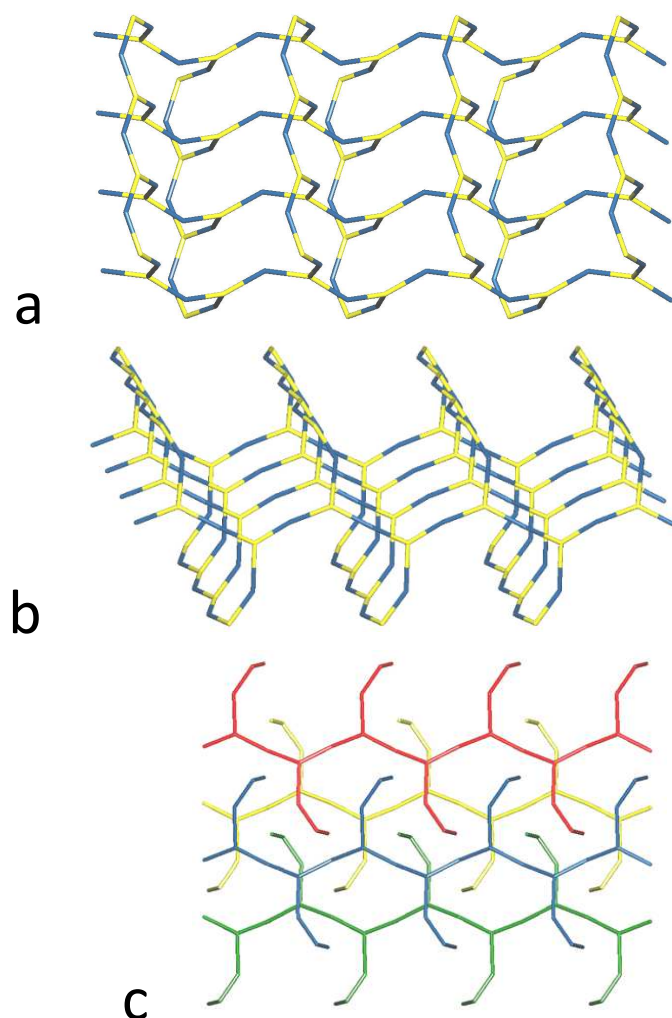


Figure 11. (a) and (b) Nodal representation of the uranyl-based 2D subunit in compound **9** (yellow, uranium; blue, centroid of dicarboxylate ligand). (c) Four of the polycatenated 2D arrays viewed edge-on.

Luminescence properties. Emission spectra under excitation at 420 nm, a value suitable for the uranyl chromophore,⁵⁵ were recorded for complexes **1–7** and **9** in the solid state (Figure 12) (A spectrum could not be obtained for complex **8** due to the contamination of the small quantity of crystals with some amorphous material). Except for complex **7** for which complete quenching of uranyl luminescence is observed, as is frequent when d-block transition metal cations are present, probably due to the latter providing a nonradiative relaxation pathway,⁵⁶ all the other spectra display the usual series of peaks associated with the vibronic progression corresponding to the $S_{11} \rightarrow S_{00}$ and $S_{10} \rightarrow S_{0\nu}$ ($\nu = 0-4$) electronic transitions.⁵⁷

Apart from some variations in the intensity of the peaks and the background, the spectra are very similar, with the positions of the maxima spanning narrow ranges of wavelengths. The four main peaks are at 481–483, 501–504, 522–525, and 542–549 nm, these positions being typical of uranyl carboxylate complexes with six equatorial donors.²³

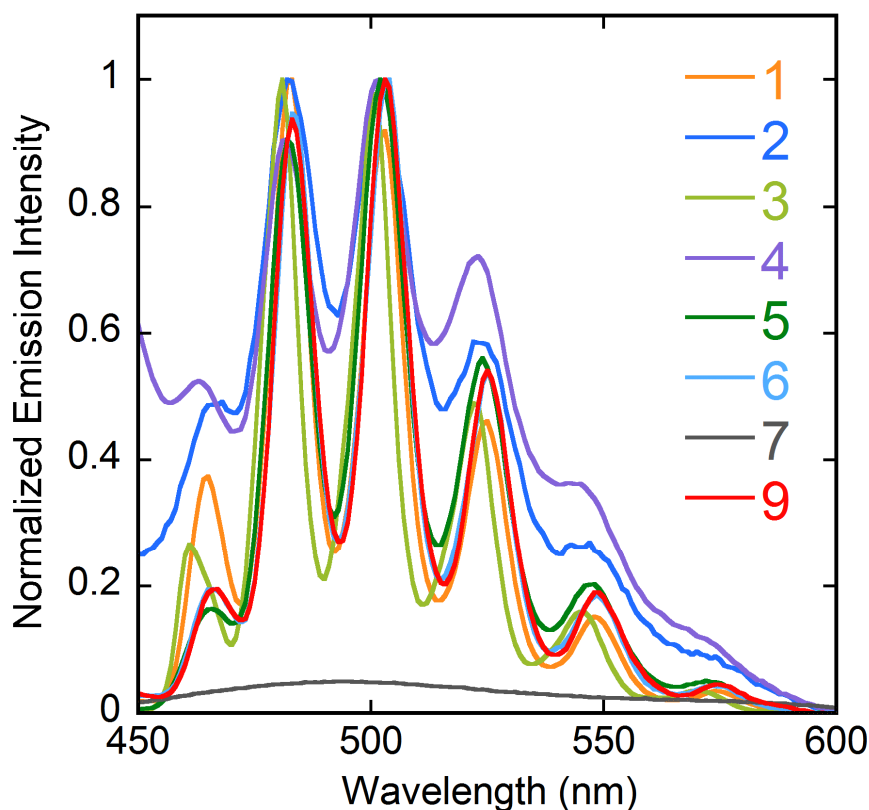


Figure 12. Emission spectra of compounds **1–7** and **9** in the solid state at room temperature, under excitation at a wavelength of 420 nm. All spectra are normalized except for that of complex **7**.

Solid-state photoluminescence quantum yields (PLQYs) have been measured in the cases for which a sufficient quantity of pure complex could be isolated. The values found are 11.5 (**1**), 3.0 (**3**), 2.5 (**4**), 3.0 (**5**), 2.0 (**6**), and 3.5% (**9**), with a standard deviation of ca. $\pm 2.5\%$. All complexes thus feature a relatively low PLQY except for complex **1**, which is 4 to 5 times more emissive (for comparison, the PLQY of uranyl nitrate hexahydrate measured under the same conditions is 24%). The last five values, for complexes **3–6** and **9**, are smaller than those previously measured in similar conditions for other uranyl carboxylate complexes, 6% for

$[\text{NH}_4][\text{PPh}_4][(\text{UO}_2)_8(c\text{-chdc})_9(\text{H}_2\text{O})_6] \cdot 3\text{H}_2\text{O}$ ($c\text{-chdcH}_2 = \text{cis-1,2-cyclohexanedicarboxylic acid}$),¹⁹ $[\text{NH}_4]_2[\text{PPh}_4]_2[(\text{UO}_2)_4(\text{ADA})_6]$, and $[\text{NH}_4]_2[\text{PPh}_3\text{Me}]_2[(\text{UO}_2)_4(\text{ADA})_6]$ ($\text{H}_2\text{ADA} = 1,3\text{-adamantanediacetic acid}$),²⁰ 9% for $[\text{H}_2\text{NMe}_2][\text{PPh}_3\text{Me}][(\text{UO}_2)_2(\text{ADA})_3] \cdot \text{H}_2\text{O}$,²⁰ and 13% for $[\text{PPh}_4]_2[(\text{UO}_2)_2(t\text{-1,4-chdc})_3] \cdot 4\text{H}_2\text{O}$ ($t\text{-1,4-chdcH}_2 = \text{trans-1,4-cyclohexanedicarboxylic acid}$).¹⁸

The relatively low PLQYs in all these cases are associated with the fact that the complexes all appear pale yellow in colour under normal sunlight, whereas the recently reported, related complexes $[\text{NMe}_4]_2[(\text{UO}_2)_4(\text{C}_2\text{O}_4)_4(\text{C4})]^{58}$ and $[\text{UO}_2(\text{HL})(\text{H}_2\text{O})]^{59}$ ($\text{H}_3\text{L} = \text{benzene-1,3,5-tricarboxylic acid}$) with room temperature quantum yields of 49 and 58%, respectively, appear green in the same light due to the greater intensity of their emission. This is also true of the complex $\text{Rb}_2[\text{UO}_2(\text{dipic})_2]$ ($\text{dipic} = \text{dipicolinate}$),⁶⁰ for which we have determined an elevated quantum yield of 42%. An enhanced quantum yield may possibly be the result of energy transfer between close luminophore units and indeed the minimum U...U distances in $[\text{NMe}_4]_2[(\text{UO}_2)_4(\text{C}_2\text{O}_4)_4(\text{C4})]$ (5.511 Å) and $[\text{UO}_2(\text{HL})(\text{H}_2\text{O})]$ (5.232 Å) are considerably shorter than those in any of the presently studied species (and shorter than that in uranyl nitrate hexahydrate of 6.09 Å). However, the minimum U...U separation in $\text{Rb}_2[\text{UO}_2(\text{dipic})_2]$ (7.517 Å) is similar to that [7.4522(7) Å] in the weakly emitting complex **6**, while that in complex **1** [7.2691(2) Å] is intermediate between the smallest [6.3902(3) Å in **4**] and the largest [8.9626(3) Å in **3**] in the present series. Another parameter that should be taken into account is the distance between the luminescent uranyl center and the electron-withdrawing phosphonium ions, which are potential photoluminescence quenchers, in complexes **1** and **3–6**. In this regard, complex **1**, which has the highest PLQY of the series, also has a minimum U...P separation of 6.8382(8) Å which is longer than any of those in complexes **3–6** [6.0169(7)–6.6330(4) Å], although the difference is rather small. However, it is no doubt an oversimplification to consider general correlations between quantum yields and such simple parameters.

CONCLUSIONS

Adding to our previous work on anionic uranyl ion complexes with α,ω -dicarboxylates using counteranions of varying bulkiness and offering different possibilities of interactions with these anions (apart from dominating Coulombic forces), we have reported here the synthesis, crystal structure and, in most cases, luminescence properties of nine new complexes. In these compounds, crystallized under solvo-hydrothermal conditions, the Cn^{2-} ligands are of medium length, with $n = 6-9$, and three families of counterions are represented: PPh_4^+/PPh_3Me^+ , macrocyclic ligand complexes of 3d-block metal cations, and, in one case, a cation, K^+ , labile with respect to its coordination sphere and flexible in its coordination geometry. Amongst other factors, there is systematic variation here in the accessibility toward lone pair donors of the centre on which the positive charge is formally located, P^+ in the phosphonium cations being inaccessible, Ni^{II} and Cu^{II} in their tetra-azamacrocyclic complexes being capable of accepting up to two extra donors in a specific stereochemistry, and K^I being completely accessible.

Overall, one-dimensional coordination polymers are the most frequent assemblies formed, being found in five complexes with PPh_4^+/PPh_3Me^+ (**1-5**) and in the complex including $[Cu(R,S-Me_6cyclam)]^{2+}$ (**7**). The prevalence of chains in this series is in contrast to the higher level of aggregation (and sometimes uranyl oligomerization) found in neutral uranyl complexes with Cn^{2-} ligands having similar n values.^{7,61} The separating effect of bulky counterions, which promotes formation of discrete, polynuclear species in other cases,^{14,19,20} may be at play here, although it must be noted that some of these other cases involve ligands with significant degrees of conformational restriction. Notwithstanding the common low dimensionality in the present instances, there is some structural variety, with simple zigzag chains including terminal nitrate coligands in **1** and **2**, curved ribbons with lateral uncomplexed carboxylic acid groups giving threefold parallel 2D interpenetrated hydrogen bonded networks in **3**, ladderlike chains in **4** and **7**, and a chain displaying an alternation of simple and double links in **5**. A heavily corrugated

honeycomb 2D assembly is found in complex **6**, with $C9^{2-}$ ligands and PPh_3Me^+ counterions. An increase in dimensionality also occurs when the counterions become part of the polymer itself, which occurs in the 2D assembly with $C7^{2-}$ ligands and $[Ni(cyclam)]^{2+}$ axially bound to two carboxylate groups (complex **8**) and in the 3D framework obtained from $C7^{2-}$ and potassium cations (**9**). The latter has the particularity of containing uranyl carboxylate subunits displaying 2D \rightarrow 3D parallel polycatenation.

Except when one carboxylic acid group retains its proton and is uncoordinated, the Cn^{2-} ligands in the present series are all bis-chelating toward uranyl, with additional bridging of two potassium cations in complex **9**, except in complex **8**, in which the bridging bidentate $\mu_2-\kappa^1O:\kappa^2O'$ mode is observed (with two uranyl or one uranyl and one nickel(II) cations as coordinated species). Thus, the variations in the geometry of the assemblies formed can be seen as reflecting both the specific nature of the non-uranyl cation and the flexibility of the aliphatic chains which can adopt a large range of conformations with variable curvature. Given the expectation that rotational barriers to conformer interconversion in polymethylene chains should be small,⁶² probably smaller than $CH\cdots O$ interaction energies⁴⁴ and certainly smaller than coordinate bond energies, priority as structure-directing influences should be given to the various interactions of the non-uranyl cations with the UO_6 entities formed by carboxylate binding. The sometimes marked differences in the interactions of similar species, such as seen between PPh_4^+ and PPh_3Me^+ or $[Cu(R,S-Me_6cyclam)]^{2+}$ and $[Ni(cyclam)]^{2+}$ in the present work, let alone differences in the pattern of interactions of a particular cation in different complexes,^{12,18,21} is, however, an indication that the predictability of cation influences is low. Nevertheless, it is notable that $[Ni(cyclam)]^{2+}$ counterions, with their ability to bind to two axial donors, appear here also as suitable linkers between essentially planar uranyl-containing subunits.²¹

In addition to the desirability of a structure containing potential reaction cavities, an important property in regard to any possible application of uranyl ion coordination polymers is their solid state PLQY. While phosphonium countercations appear to have an advantage over transition metal species in that they do not lead to complete luminescence quenching, the PLQY values obtained in the several systems we have investigated are all relatively low and the structural factors which need to be optimized to obtain higher values remain somewhat obscure. Replacement of the phenyl groups on phosphorus with large saturated substituents, however, is a strategy which the present results indicate may be worthy of pursuit.

ASSOCIATED CONTENT

Accession Codes

CCDC 1869722–1869730 contain the supplementary crystallographic data for this paper. These data can be obtained free of charge via www.ccdc.cam.ac.uk/data_request/cif, or by emailing data_request@ccdc.cam.ac.uk, or by contacting The Cambridge Crystallographic Data Centre, 12 Union Road, Cambridge CB2 1EZ, UK; fax: +44 1223 336033.

AUTHOR INFORMATION

Corresponding Authors

*E-mail: pierre.thuery@cea.fr. (P.T.)

*E-mail: harrowfield@unistra.fr. (J.H.)

ORCID

Pierre Thuéry: [0000-0003-1683-570X](https://orcid.org/0000-0003-1683-570X)

Youssef Atoini: [0000-0003-4851-3713](https://orcid.org/0000-0003-4851-3713)

Jack Harrowfield: [0000-0003-4005-740X](https://orcid.org/0000-0003-4005-740X)

Notes

The authors declare no competing financial interest.

REFERENCES

1. Wang, K. X.; Chen, J. S. Extended Structures and Physicochemical Properties of Uranyl–Organic Compounds. *Acc. Chem. Res.* **2011**, *44*, 531–540.
2. Andrews, M. B.; Cahill, C. L. Uranyl Bearing Hybrid Materials: Synthesis, Speciation, and Solid-State Structures. *Chem. Rev.* **2013**, *113*, 1121–1136.
3. Loiseau, T.; Mihalcea, I.; Henry, N.; Volkringer, C. The Crystal Chemistry of Uranium Carboxylates. *Coord. Chem. Rev.* **2014**, *266–267*, 69–109.
4. Su, J.; Chen, J. S. MOFs of Uranium and the Actinides. *Struct. Bond.* **2015**, *163*, 265–296.
5. Thuéry, P.; Harrowfield, J. Recent Advances in Structural Studies of Heterometallic Uranyl-Containing Coordination Polymers and Polynuclear Closed Species. *Dalton Trans.* **2017**, *46*, 13660–13667.
6. Groom, C. R.; Bruno, I. J.; Lightfoot, M. P.; Ward, S. C. The Cambridge Structural Database. *Acta Crystallogr., Sect. B* **2016**, *72*, 171–179.
7. Borkowski, L. A.; Cahill, C. L. Crystal Engineering with the Uranyl Cation I. Aliphatic Carboxylate Coordination Polymers: Synthesis, Crystal Structures, and Fluorescent Properties. *Cryst. Growth Des.* **2006**, *6*, 2241–2247.
8. Borkowski, L. A.; Cahill, C. L. Crystal Engineering with the Uranyl Cation II. Mixed Aliphatic Carboxylate/Aromatic Pyridyl Coordination Polymers: Synthesis, Crystal Structures, and Sensitized Luminescence. *Cryst. Growth Des.* **2006**, *6*, 2248–2259.

9. Kerr, A. T.; Cahill, C. L. Crystal Engineering with the Uranyl Cation III. Mixed Aliphatic Dicarboxylate/Aromatic Dipyridyl Coordination Polymers: Synthesis, Structures, and Speciation. *Cryst. Growth Des.* **2011**, *11*, 5634–5641.
10. Thuéry, P. Uranyl Ion Complexation by Aliphatic Dicarboxylic Acids in the Presence of Cucurbiturils as Additional Ligands or Structure-Directing Agents. *Cryst. Growth Des.* **2011**, *11*, 2606–2620.
11. Thuéry, P.; Harrowfield, J. Anchoring Flexible Uranyl Dicarboxylate Chains through Stacking Interactions of Ancillary Ligands on Chiral U(VI) Centres. *CrystEngComm* **2016**, *18*, 3905–3918.
12. Thuéry, P.; Rivière, E.; Harrowfield, J. Counterion-Induced Variations in the Dimensionality and Topology of Uranyl Pimelate Complexes. *Cryst. Growth Des.* **2016**, *16*, 2826–2835.
13. Thuéry, P.; Harrowfield, J. The Crystalline α,ω -Dicarboxylate Metal Complex with the Longest Aliphatic Chain to Date: Uranyl 1,15-Pentadecanedioate. *Dalton Trans.* **2017**, *46*, 13677–13680.
14. Thuéry, P.; Harrowfield, J. A New Form of Triple-Stranded Helicate Found in Uranyl Complexes of Aliphatic α,ω -Dicarboxylates. *Inorg. Chem.* **2015**, *54*, 10539–10541.
15. Thuéry, P. From Helicates to Borromean Links: Chain Length Effect in Uranyl Ion Complexes of Aliphatic α,ω -Dicarboxylates. *Cryst. Growth Des.* **2016**, *16*, 546–549.
16. Thuéry, P.; Harrowfield, J. Uranyl Ion Complexes with Long-Chain Aliphatic α,ω -Dicarboxylates and 3d-Block Metal Counterions. *Inorg. Chem.* **2016**, *55*, 2133–2145.
17. Thuéry, P.; Harrowfield, J. Ag^I and Pb^{II} as Additional Assembling Cations in Uranyl Coordination Polymers and Frameworks. *Cryst. Growth Des.* **2017**, *17*, 2116–2130.
18. Thuéry, P.; Atoini, Y.; Harrowfield, J. Uranyl–Organic Coordination Polymers with *trans*-1,2-, *trans*-1,4-, and *cis*-1,4-Cyclohexanedicarboxylates: Effects of Bulky PPh₄⁺ and PPh₃Me⁺ Counterions. *Cryst. Growth Des.* **2018**, *18*, 2609–2619.

19. Thuéry, P.; Atoini, Y.; Harrowfield, J. Counterion-Controlled Formation of an Octanuclear Uranyl Cage with *cis*-1,2-Cyclohexanedicarboxylate Ligands. *Inorg. Chem.* **2018**, *57*, 6283–6288.
20. Thuéry, P.; Atoini, Y.; Harrowfield, J. Closed Uranyl–Dicarboxylate Oligomers: A Tetranuclear Metallatricycle with Uranyl Bridgeheads and 1,3-Adamantanediacetate Linkers. *Inorg. Chem.* **2018**, *57*, 7932–7939.
21. Thuéry, P.; Harrowfield, J. [Ni(cyclam)]²⁺ and [Ni(*R,S*-Me₆cyclam)]²⁺ as Linkers or Counterions In Uranyl–Organic Species with *cis*- and *trans*-1,2-Cyclohexanedicarboxylate Ligands. *Cryst. Growth Des.* **2018**, *18*, 5512–5520.
22. Thuéry, P.; Atoini, Y.; Harrowfield, J. Crown Ethers and Their Alkali Metal Ion Complexes as Assembler Groups in Uranyl–Organic Coordination Polymers with *cis*-1,3-, *cis*-1,2-, and *trans*-1,2-Cyclohexanedicarboxylates. *Cryst. Growth Des.* **2018**, *18*, 3167–3177.
23. Thuéry, P.; Harrowfield, J. Structural Consequences of 1,4-Cyclohexanedicarboxylate Cis/Trans Isomerism in Uranyl Ion Complexes: From Molecular Species to 2D and 3D Entangled Nets. *Inorg. Chem.* **2017**, *56*, 13464–13481 and references therein.
24. Liu, C.; Chen, F. Y.; Tian, H. R.; Ai, J.; Yang, W.; Pan, Q. J.; Sun, Z. M. Interpenetrated Uranyl–Organic Frameworks with *bor* and *pts* Topology: Structure, Spectroscopy, and Computation. *Inorg. Chem.* **2017**, *56*, 14147–14156.
25. Wang, S.; Mei, L.; Yu, J. P.; Hu, K. Q.; Liu, Z. R.; Chai, Z. F.; Shi, W. Q. Large-Pore Layered Networks, Polycatenated Frameworks, and Three-Dimensional Frameworks of Uranyl Tri(biphenyl)amine/Tri(phenyl)amine Tricarboxylate: Solvent-/Ligand-Dependent Dual Regulation. *Cryst. Growth Des.* **2018**, *18*, 4347–4356.
26. Zhang, X. L.; Hu, K. Q.; Mei, L.; Zhao, Y. B.; Wang, Y. T.; Chai, Z. F.; Shi, W. Q. Semirigid Tripodal Ligand Based Uranyl Coordination Polymer Isomers Featuring 2D Honeycomb Nets. *Inorg. Chem.* **2018**, *57*, 4492–4501.

27. Tait, A. M.; Busch, D. H., in *Inorganic Syntheses*, Vol. 18; Douglas, B. E., (Vol. Ed.); John Wiley & Sons: New York, 1978; Chapter 1.2, p 10.
28. Clay, R.; Murray-Rust, J.; Murray-Rust, P. An X-Ray Structural and Thermodynamic Investigation of the Blue and Red Forms of (C-meso-5,5,7,12,12,14-Hexamethyl-1,4,8,11-tetraazacyclotetradecane)copper(II) Perchlorate. *J. Chem. Soc., Dalton Trans.* **1979**, 1135–1139.
29. Hooft, R. W. W. *COLLECT*, Nonius BV: Delft, The Netherlands, 1998.
30. Otwinowski, Z.; Minor, W. Processing of X-Ray Diffraction Data Collected in Oscillation Mode. *Methods Enzymol.* **1997**, 276, 307–326.
31. Sheldrick, G. M. SHELXT – Integrated Space-Group and Crystal-Structure Determination. *Acta Crystallogr., Sect. A* **2015**, 71, 3–8.
32. Sheldrick, G. M. Crystal Structure Refinement with SHELXL. *Acta Crystallogr., Sect. C* **2015**, 71, 3–8.
33. Farrugia, L. J. WinGX and ORTEP for Windows: an Update. *J. Appl. Crystallogr.* **2012**, 45, 849–854.
34. Momma, K.; Izumi, F. VESTA: a Three-Dimensional Visualization System for Electronic and Structural Analysis. *J. Appl. Crystallogr.* **2008**, 41, 653–658.
35. Blatov, V. A. *TOPOS*; Samara State University: Samara, Russia, 2004.
36. Spek, A. L. Structure Validation in Chemical Crystallography. *Acta Crystallogr., Sect. D* **2009**, 65, 148–155.
37. Thuéry, P.; Harrowfield, J. Modulation of the Structure and Properties of Uranyl Ion Coordination Polymers Derived from 1,3,5-Benzenetriacetate by Incorporation of Ag(I) or Pb(II). *Inorg. Chem.* **2016**, 55, 6799–6816 and references therein.
38. Thuéry, P.; Harrowfield, J. Structural Variations in the Uranyl/4,4'-Biphenyldicarboxylate System. Rare Examples of 2D → 3D Polycatenated Uranyl–Organic Networks. *Inorg. Chem.* **2015**, 54, 8093–8102 and references therein.

39. Andrews, M. B.; Cahill, C. L. *In Situ* Oxalate Formation during Hydrothermal Synthesis of Uranyl Hybrid Materials. *CrystEngComm* **2011**, *13*, 7068–7078.
40. Knope, K. E.; Kimura, H.; Yasaka, Y.; Nakahara, M.; Andrews, M. B.; Cahill, C. L. Investigation of *in Situ* Oxalate Formation from 2,3-Pyrazinedicarboxylate under Hydrothermal Conditions Using Nuclear Magnetic Resonance Spectroscopy. *Inorg. Chem.* **2012**, *51*, 3883–3890.
41. Spackman, M. A.; Jayatilaka, D. Hirshfeld Surface Analysis. *CrystEngComm* **2009**, *11*, 19–32.
42. Wolff, S. K.; Grimwood, D. J.; McKinnon, J. J.; Turner, M. J.; Jayatilaka, D.; Spackman, M. A. *CrystalExplorer*; University of Western Australia: Crawley, Australia, 2012.
43. Taylor, R.; Kennard, O. Crystallographic Evidence for the Existence of C–H···O, C–H···N, and C–H···Cl Hydrogen Bonds. *J. Am. Chem. Soc.* **1982**, *104*, 5063–5070.
44. Desiraju, G. R. The C–H···O Hydrogen Bond: Structural Implications and Supramolecular Design. *Acc. Chem. Res.* **1996**, *29*, 441–449.
45. Scudder, M.; Dance, I. Crystal Supramolecular Motifs. Two- and Three-Dimensional Networks of Ph₄P⁺ Cations Engaged in Sixfold Phenyl Embraces. *J. Chem. Soc., Dalton Trans* **1998**, 3167–3175, and references therein.
46. Etter, M. C.; MacDonald, J. C.; Bernstein, J. Graph-Set Analysis of Hydrogen-Bond Patterns in Organic Crystals. *Acta Crystallogr., Sect. B* **1990**, *46*, 256–262.
47. Bernstein, J.; Davis, R. E.; Shimon, L.; Chang, N. L. Patterns in Hydrogen Bonding: Functionality and Graph Set Analysis in Crystals. *Angew. Chem. Int. Ed.* **1995**, *34*, 1555–1573.
48. Novikov, S. A.; Grigoriev, M. S.; Serezhkina, L. B.; Serezhkin, V. N. Potassium and Magnesium Succinatouranilates – Synthesis and Crystal Structure. *J. Solid State Chem.* **2017**, *248*, 178–182.

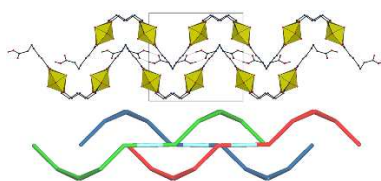
49. Benetollo, F.; Bombieri, G.; Herrero, J. A.; Rojas, R. M. Preparation, Properties and Crystal Structure of Lithium Glutarate Hydrogenlutarate Dioxouranate(VI) Tetrahydrate $\text{UO}_2(\text{C}_5\text{H}_6\text{O}_4)\text{Li}(\text{C}_5\text{H}_7\text{O}_4)\cdot 4\text{H}_2\text{O}$. *J. Inorg. Nucl. Chem.* **1979**, *41*, 195–199.
50. Novikov, S. A.; Serezhkina, L. B.; Grigor'ev, M. S.; Manakov, N. V.; Serezhkin, V. N. Crystal Structures of New Uranyl Glutarate Coordination Polymers $(\text{NH}_4)_2[(\text{UO}_2)_2(\text{glt})_3]\cdot n\text{H}_2\text{O}$ ($n = 3$ or 6) and $\text{R}[\text{UO}_2(\text{glt})(\text{Hglt})]\cdot \text{H}_2\text{O}$ ($\text{R} = \text{Na}, \text{K}, \text{Rb}$ or Cs). *Polyhedron* **2016**, *117*, 644–651.
51. Zehnder, R. A.; Boncella, J. M.; Cross, J. N.; Kozimor, S. A.; Monreal, M. J.; La Pierre, H. S.; Scott, B. L.; Tondreau, A. M.; Zeller, M. Network Dimensionality of Selected Uranyl(VI) Coordination Polymers and Octopus-like Uranium(IV) Clusters. *Cryst. Growth Des.* **2017**, *17*, 5568–5582.
52. Novikov, S. A.; Serezhkina, L. B.; Grigoriev, M. S.; Serezhkin, V. N. Mg, Ca and Ba Glutaratouranylates – Synthesis and Structure. *Polyhedron* **2018**, *141*, 147–152.
53. Whiteside, A.; Xantheas, S. S.; Gutowski, M. Is Electronegativity a Useful Descriptor for the Pseudo-Alkali Metal NH_4 ? *Chem. Eur. J.* **2011**, *17*, 13197–13205.
54. Thuéry, P.; Harrowfield, J. Tetrahedral and Cuboidal Clusters in Complexes of Uranyl and Alkali or Alkaline-Earth Metal Ions with *rac*- and *(1R,2R)*-*trans*-1,2-Cyclohexanedicarboxylate. *Cryst. Growth Des.* **2017**, *17*, 2881–2892.
55. Knope, K. E.; de Lill, D. T.; Rowland, C. E.; Cantos, P. M.; de Bettencourt-Dias, A.; Cahill, C. L. Uranyl Sensitization of Samarium(III) Luminescence in a Two-Dimensional Coordination Polymer. *Inorg. Chem.* **2012**, *51*, 201–206.
56. Kerr, A. T.; Cahill, C. L. Postsynthetic Rearrangement/Metalation as a Route to Bimetallic Uranyl Coordination Polymers: Syntheses, Structures, and Luminescence. *Cryst. Growth Des.* **2014**, *14*, 1914–1921.

57. Brachmann, A.; Geipel, G.; Bernhard, G.; Nitsche, H. Study of Uranyl(VI) Malonate Complexation by Time Resolved Laser-Induced Fluorescence Spectroscopy (TRLFS). *Radiochim. Acta* **2002**, *90*, 147–153.
58. Xie, J.; Wang, Y.; Liu, W.; Lin, X.; Chen, L.; Zou, Y.; Diwu, J.; Chai, Z.; Albrecht-Schmitt, T. E.; Liu, G.; Wang, S. Highly Sensitive Detection of Ionizing Radiations by a Photoluminescent Uranyl Organic Framework. *Angew. Chem. Int. Ed.* **2017**, *56*, 7500–7504.
59. Wang, Y.; Yin, X.; Liu, W.; Xie, J.; Chen, J.; Silver, M. A.; Sheng, D.; Chen, L.; Diwu, J.; Liu, N.; Chai, Z.; Albrecht-Schmitt, T. E.; Wang, S. Emergence of Uranium as a Distinct Metal Center for Building Intrinsic X-ray Scintillators. *Angew. Chem. Int. Ed.* **2018**, *57*, 7883–7887.
60. Harrowfield, J. M.; Lugan, N.; Shahverdizadeh, G. H.; Soudi, A. A.; Thuéry, P. Solid State Luminescence and π -Stacking in Crystalline Uranyl Dipicolinates. *Eur. J. Inorg. Chem.* **2006**, 389–396.
61. Borkowski, L. A.; Cahill, C. L. Topological Evolution in Uranyl Dicarboxylates: Synthesis and Structures of One-Dimensional $\text{UO}_2(\text{C}_6\text{H}_8\text{O}_4)(\text{H}_2\text{O})_2$ and Three-Dimensional $\text{UO}_2(\text{C}_6\text{H}_8\text{O}_4)$. *Inorg. Chem.* **2003**, *42*, 7041–7045.
62. Eliel, E. L.; Wilen, S. H. Stereochemistry of Organic Compounds. Wiley India, 2008.

For Table of Contents Use Only

**Structure-Directing Effects of Counterions in Uranyl Ion
Complexes with Long-Chain Aliphatic α,ω -Dicarboxylates:
1D to Polycatenated 3D Species**

Pierre Thuéry, Youssef Atoini and Jack Harrowfield



Nine uranyl ion complexes with aliphatic dicarboxylate ligands were synthesized with diverse counterions, the latter inducing different polymeric arrangements, either one-, two- or three-dimensional. Two compounds contain entangled nets, hydrogen bonded, two-dimensional interpenetrated in one case, and two-dimensional polycatenated in the other.